REDUCTION OF FRICTIONAL RESISTANCE CAUSED BY SINGLE AND COMBINED ADDITIVES

A Thesis
Submitted to the College of Engineering
of Nahrain University in Partial Fulfillment
of the Requirements for the Degree of
Master of Science
in
Chemical Engineering

by

OMAR JALAA YAHYA

B.Sc. in Chemical Engineering 2006

Jummada II 1430
June 2009

Certification

I certify that this thesis entitled “**Reduction of Frictional Resistance Caused by Single and Combined Additives**” was prepared by **Omar Jalaa Yahya** under my supervision at Nahrain University / College of Engineering in partial fulfillment of the requirements for the degree of Master of Science in Chemical Engineering.

Signature: J. Shanshool
Name : **Prof. Dr. Jabir Shanshool**
(Supervisor)

Date: 15 / 6 / 2009

Signature:
Name: **Prof. Dr. Qasim J. Slaiman**
(Head of department)

Date: / / 2009

Certificate

We certify, as an examining committee, that we have read this thesis entitled " **Reduction of Frictional Resistance Caused by Single and Combined Additives**”, examined the student **Omar Jalaa Yahya** in its content and found it meets the standard of thesis for the degree of Master of Science in Chemical Engineering.

Signature: J. Shanshool
Name: **Prof. Dr. Jabir Shanshool**
(Supervisor)
Date: / / 2009

Signature:
Name: **Dr.Khalid M. Mousa**
(Member)
Date: / / 2009

Signature:
Name: **Dr. Cecilia Kh. Haweel**
(Member)
Date: 16 / 6 / 2009

Signature: T. Kashmoula
Name: **Dr. Talib Bahjat Kashmoula**
(Chairman)
Date: / / 2009

Approval of the College of Engineering

Signature: M. J. JWeeg
Name: **Prof. Dr. Muhsin J. Jweeg**
(Dean)
Date: 5 / 7 / 2009

Abstract

The experimental study was primary designed to evaluate the effectiveness of various additive types as drag-reducer agents, both in the single and binary mixed forms. Since a comparison between more than one additives type, especially between water soluble polymers and suspended particles are rare in literature .The additives, which have been investigated in present work, were Polyethylene Oxide (PEO) and Polyacrylamide (PAAM) up to 100 ppm, as flexible, long chain, synthetic polymers and Xanthan Gum (XG) up to 200 ppm, as a rigid natural polysaccharide polymer .Furthermore, a certain type of natural Clay (Kaolin) wasconcluded as suspended particles additive up to 1000 ppm, in addition to Aluminum Sulfate (Alum) up to 500 ppm, and Trisodium polyphosphate (STPP) were investigated, up to 200 ppm, in the present investigation. Alum and STPP were used for first time as drag reducing agents.

The drag-reduction efficiency of the flexible polymers, PEO and PAAM is larger than that of other used additives in a whole concentration range at different flowing velocities A maximum drag-reduction of about 32% has been achieved when 100 ppm PEO and PAAM were added at 6.0 m^3/hr flow rate, these it has been considered as an optimum one between the other types of additive. Xanthan Gum, Clay, and Trisodium polyphosphate showed a moderate efficiency as drag-reducer additives .While, Alum was more efficient at concentrations 500-1000 ppm, which gave 21-25% drag-reduction probably, due to form colloid with water, which causes lowering the solution viscosity.

A slight increase of drag-reduction was observed by mixing of Clay, Alum or STPP with PEO and PAAM, while, a significant enhancement of drag-reduction ability for Xanthan Gum was obtained by mixing with Clay, Alum or STPP combined additives.

Friction factor values were calculated from experimental data observed for all considered additives at different flowing conditions. Friction factor lines for Polyethylene Oxide, Polyacrylamide and Alum at high Reynolds number positioned towards Virk asymptote, which was never reached .

List of Contents

Contents **Page**

Abstract I

List of Contents III

Notations V

List of Tables VIII

List of Figures IX

CHAPTER ONE
INTRODUCTION

1.1 Introduction 1

CHAPTER TWO
LITERATURE SURVEY

2.1 Drag -Reduction Phenomenon: 4

2.2 Drag Reducer Additives 6

2.2.1 Polymers 6

2.2.2 Surfactant 9

2.2.3 Suspended particles 14

2.3 Microbubbles 15

2.4 Compliant Coatings 17

2.4.1 Overview 17

2.4.2 Coating Optimization 18

2.5 Hypothetical Mechanism 21

2.6 Friction 23

2.6.1 Fundamentals 23

2.6.2 Friction Factor 29

CHAPTER THREE
EXPERIMENTER WORK

3.1 Materials 32

3.2 Preparation of additives solutions 32
3.3 Flow Loop 33
3.4 Experimental Procedure 36
3.5 Calculations 37

CHAPTER FOUR
RESULTS AND DISCUSSION

4.1 Introduction 38
4.2 Polymeric Additives 40
4.2.1 Concentration Effect 40
4.2.2 Flow Rate Effect 42
4.3 Trisodium Polyphosphate 45
4.4 Suspended Particles Additives 47
4.4.1 Clay (Kaolin) 47
4.4.2 Alum 49
4.5 Effectiveness of Binary Additives 52
4.5.1 Polymers and Clay 52
4.5.2 Polymer and Alum 55
4.5.3 Binary mixtures with STPP 58
4.6 Friction Factor 61

CHAPTER FIVE
CONCLUSIONS AND RECOMMENDATIONS

5.1 Conclusions 65
5.2 Recommendations 66

REFERENCES 67

APPENDICES

Appendix A A-1
Appendix B B-1

Notations

Variable Notations

Symbols	**Description**	**Unit**
C	Additives concentration	ppm
CMC	Critical micelle concentration	Mol/dm^3
D	Pipe inside diameter	m
%Dr	Percentage drag reduction	[-]
%Dri	Percentage drag reduction increase	[-]
h_f	Head loss	m
H_p	Horse power	
L	Testing section length	m
M_w	Molecular weight	g/g mole
ΔP	Pressure drop	N/m^2
Q	Volumetric flow rate	m^3/hr
Re	Reynolds number	[-]
T	Temperature	°C
U	Mean velocity	m/s

Abbreviations

Abbreviations	**Definition**
Na-CMC	SoduimCarboxymethylcellulose
CTAB	Cetryltrimethylammonium Bromide
CTAC	Cetryltrimethylammonium Chloride
DRA	Drag Reduction Agent
GG	Gear Gum
HEC	Hydroxyethylecellulose
MDRA	Maximum Drag Reduction Asymptote
PAAM	Polyacrylamide
PCIP	Polycisisoprene
PDMS	Polydimethylsiloxane
PEO	Polyethylene Oxide
PIB	Polyisobutylene
PMMA	Polymethylmethacrylate
PS	Polystyrene
SDBS	Sodium Dodecyl Banzene
SLES	Sodium Lauryl Sulfate
STAC	Stearyltrimethylammoniym chloride
TSW	TollmienSchlichting Wave

Greek Symbols

Symbols	**Description**	**Unit**
ΔP	Pressure drop	N/m^2
ΔP_a	Pressure drop after adding the additive	N/m^2
ΔP_b	Pressure drop before adding the additive	N/m^2
ρ	Fluid density	kg/m^3
τ_w	Wall shear stress	N/m^2
f	Fanning friction factor	
μ	Dynamic viscosity	Pa.s , poise
υ	Kinematicviscosity	c.st
ε	Roughness of pipe	m

List of Tables

Table	**Title**	**Page**
2.1	Drag – reducing polymer additive	7

List of Figures

Figure	Title	Page
2.1	Effect of pipe diameter on friction factors of equimolar HDTAB, 1 – Naphthol solution	11
2.2	Schematic of the compliant wall, a)single layer and b)double layer	19
2.3	Detail of compliant coating	20
2.4	Hypothetical mechanism of drag reduction	22
2.5	Pipe friction chart φ verses Re	25
3.1	Shaker	33
3.2	Schematic diagram of experimental rig	34
3.3	Calibration of flow meter	35
4.1	pressure drop vs .flow rate of water without treatment	39
4.2	Percent drag-reduction vs .concentrations for different flow rates for Poly(ethelenoxide)PEO	41
4.3	Percent drag-reduction vs .concentrations for different flow rates for polyacrylamide (PAAM)	41
4.4	Percent drag-reduction vs .concentrations for different flow rates for Xanthan Gum (XG)	42
4.5	Percent drag reduction vs .flow rate for three selected concentration of Poly(ethelenoxide)PEO	43
4.6	Percent drag reduction vs .flow rate for three selected concentration of polyacrylamide (PAAM)	44
4.7	Percent drag reduction vs .flow rate for four selected concentration of Xanthan Gum (XG)	44
4.8	Percent drag reduction vs .flow rate for different concentrations of STPP	45

4.9	Effect of flow rate on percentage drag-reduction of 200 ppm STPP additive	46
4.10	Percent drag reduction vs .Clay concentration of different flow rates	48
4.11	Effect of flow rate on effectiveness of Clay as drag-reduction agent	49
4.12	Percent drag reduction vs .flow rate for different concentrations of Alum	50
4.13	Percent drag reduction vs .concentrations for different flow rates of Alum	51
4.14	Percent drag reduction vs .flow rate for 50 ppm of PEO combined with different concentrations of Clay	53
4.15	Percent drag reduction vs .flow rate for 50 ppm of PAAM combined with different concentrations of Clay	53
4.16	Percent drag reduction vs .flow rate for 50 ppm of XG combined with different concentrations of Clay	54
4.17	Percent drag reduction increase vs .concentration of clay for different polymers at 6m^3/hr	54
4.18	Percent drag reduction vs .flow rate for different concentrations of Alum at 50 ppm PEO	56
4.19	Percent drag reduction vs .flow rate for different concentrations of Alum at 50 ppm PAAM	56
4.20	Percent drag reduction vs .flow rate for different concentrations of Alum at 100 ppm XG	57
4.21	Percent drag reduction increase vs .concentrations of Alum for different Polymers at 6 m^3/hr	57

4.22	Percent drag reduction vs .flow rate for 100 ppm Xanthan Gum (XG)and different concentrations of (STPP)	58
4.23	Percent drag reduction increase vs .concentrations for 100 ppm XG and different concentrations of STPP at $6m^3/hr$	59
4.24	Percent drag reduction vs .flow rate for 200 ppm of STPP and different concentration of Alum	60
4.25	Percent drag reduction increase vs .concentrations for 200 ppm STPP and different concentrations of Alum at $6m^3/hr$	61
4.26	the fanning friction factor vs .Reynolds number for polymers, STPP, Alum, and Clay	63
4.27	the fanning friction factor vs .Reynolds number for PEO mixed with Alum and Clay	63
4.28	the fanning friction factor vs .Reynolds number for PAAM mixed with Alum and Clay	64

CHAPTER ONE

INTRODUCTION

1.1 Introduction:

Turbulent flows can occur in the boundary layer near solid surfaces and the associated friction increases, as the flow velocity increases. The energy losses and self-noise due to turbulence friction can be of very high magnitude. This necessitates unabated research into drag reduction. The main purpose of drag reduction (DR) is to delay the onset of turbulent flows. In other words, a drag reducer will shift the transition from a laminar flow to a turbulent flow at higher flow velocity. In 1949, Toms (1) reported unusually low friction factors for dilute solutions of poly(methyl methacrylate) in monochlorobenzene. He was the first to publish drag reduction data which was later named as the “Toms effect”. In the late fifties and early sixties, the effect of dilute polymer solutions on drag reduction was actively investigated. Possible defense application was initiated by the work of Pruitt and Crawford (2) and Savins (3). Hoyt and coworkers (4-7) from U. S. Navy organizations have made significant contributions to the drag properties of the dilute solutions of poly (ethylene oxide).

Various drag- reduction agents are available, such as flexible long-chain macromolecules, colloidal surfactants and suspension of fine, insoluble fibers or particles. Among these, macromolecules, which posses a linear flexible structure and a very high molecular weight, have been widely investigated as drag reducers (8).

Power saving is the major concern of all the investigations involved in what is called "Drag Reduction Field". Reducing drag of transport field through pipelines caused by friction and turbulence losses has great benefit from economical point of view. Drag reduction may accrue using different technologies with different type of materials (8). In liquid transportation through pipelines, the addition of small amount of chemical additions (generally Polymers or Surfactants) to the flowing liquid in turbulent mode, will lead to the reduction in pressure drop which is a clue about the power saving made in the system. Another technique for drag reduction was suggested. This technique depends on adding small amount of solid particles to flowing liquid in turbulent manner through pipelines. The addition of these particles vanishes one of the major assertions in the drag reduction technique by chemical addition which is "Solubility of the addition the transported liquid", or have the water, condition that the drag reducer must be soluble or at least has the ability to penetrate or its molecules reorient in the transported liquid to be affected. This behavior suggested new and merely independent mechanism to explain the behavior (8).

The reheological characteristics of drag- reducing polymeric solution are not only quite complex, they are generally difficult to evaluate quantitatively because of the low concentration of a polymeric solution. These properties are coupled with the complex system which is virtually difficult to analyze precisely. Consequently, various approximation and simplifying assumptions are necessary in order to obtain a relationship between observable quantities (9).

The present work is an attempt at gaining some experimental data in performance of various drag-reducing additives. Therefore, tow water-soluble flexible synthetic polymers, Polyethylene Oxide and Polyacrylamide and a rigid, natural Polysach oxide, Xanthan Gum agent in addition to Trisodium polyphosphate (STPP) are included in the investigation. Furthermore a certain clay type is used as additives. Trisodium polyphosphate (STPP) and Alum are considered for the first time as drag-reducing agent.

A further object of present study is to investigate the effectiveness of mixes two additive types as drag-reducing agents.

The performed experimental data aim at showing the effect of additive concentration and solution flow rate on the drag-reduction of turbulent water flow.

CHAPTER TWO

LITERATURE SURVEY

2.1: Drag- Reduction Phenomenon:

Turbulent drag reduction which is a drastic reduction of frictional resistance can be easily observed by injection a minute amount of polymeric additives in turbulent flow (10), polymer solutions undergoing a turbulent flow in a pipe there by require a lower pressure drop to maintain the same volumetric flow rate. The addition of small amounts of additives to the flowing fluids can show significant effect on a lot of flow types, including the stability of laminar flow, transition to turbulence, vortex formation and break – up (11).

The phenomenon of drag reduction by polymer additives is very interesting from a fundamental fluid dynamics point of view. The fact that such small changes in the fluid can so drastically alter the turbulent flow characteristics strongly hints at the existence of a key mechanism of turbulence transport with which polymer interface. This means that a study of polymeric drag reduction could help in gaining more knowledge about the turbulence itself (12).

Drag reduction occurs as a result of interaction between additive molecules and coherent structures resulting from turbulent flow. Therefore, understanding and optimization of the drag reduction phenomena require a previous knowledge and understanding of turbulence in fluid flow. In addition to that, and in order to have a clear idea about the effectiveness and performance of drag reducing agents, it is essential to study the polymeric additive types (12).Drag reduction phenomenon exhibited by many Newtonian and pseudo plastic solutions , gells and suspensions , and it can be considered as a departure from their "normal" viscous behaviour in general.

Drag reduction in fluid flow is an interesting phenomenon and has widely attention from theoretical as well as practical point of view. Liquids are mostly transported through pipes, and drag reduction by adding small amount of additives can offer large economic advantages and more effectiveness of flow capacities. Consideration of throughput increase which can be either being permanent or seasonal Drag reduction offer the best quick temporary solution to such problem. Its main advantage is that no capital investment is required (13).

The addition of drag reducing additive is done by two different methods resulting in two different types of drag reduction, homogenous and heterogeneous (14). The homogenous drag reduction is done by dissolving the polymer in fluid before the experiment take place, and the second is the heterogeneous drag reduction which occurs by injection of concentrated polymer into turbulent pipe flow (14).

Polymeric drag reduction is interesting in many ways and this is reflected in the virtual explosion of research and development work in many countries on the subject during the last four decades. A vast amount of publications has appeared the majority of which concern measurements. Some of the papers are theoretical reflections, and also a respectable number of survey articles have been published. Despite this wealth of information, it cannot be said that the phenomenon is well understood. The physical mechanism responsible for the drag reduction remains largely unclear. This is caused by the fact that not only it is necessary to consider the turbulence processes that are present in the flow, but also the influence of the rheological properties of the fluid (14).

2.2 Drag Reducer Additives

2.2.1. Polymers

The polymeric drag reduction has shown much promise in reducing the energy requirement of crude oil and water transport through pipes than other types of drag reducing agents. This implies that fluid containing dilute polymer solutions, which posses a linear flexible structure and very high molecular weight, requires a lower pressure drop than pure solvent to maintain the same flow rate in a pipe (15).

When polymeric drag reducer is mixed with fluid in a pipeline, it changes the flow characteristic and reduces the turbulence. By reducing turbulent in the flow, polymer drag reducer directs more energy to moving additional fluid through the system. Studies have shown that the number of turbulent bursts originating at the pipe wall and strength of turbulent eddies are reduced by addition of polymeric drag reducer. It should be emphasized that polymeric drag reducer does not work by being absorbed into or coating the walls of the pipes, as some have thought, whereas it is dissolved into and becomes part of the fluid, not the pipe (15).

Drag reducer polymers are classified into two groups , water – soluble and oil soluble polymers , as listed in table 2.1 (15).

Table 2.1 Drag – reducing polymer additive (16)

Water soluble	Hydrocarbon soluble
Polyacrylamide (PAAM)	Polyisobutylene (PIB)
Polyethylene Oxide (PEO)	Polyethylene Oxide (PEO)
Guar gum (GG)	Polymethylmethacrylate (PMMA)
Xanthan gum (XG)	Polydimethylsiloxane (PDMS)
Soduim carboxymethylcellulose (Na-CMC)	Polycisisoprene (PCIP)
Hydroxyethylecellulose (HEC)	Polystyrene (PS)

Effective polymeric drag reduction additives are considered to be flexible, linear with high molecular weight (16) such as polyethylene oxide(17), polyacrylamid and polyisobutylene. These polymers are limited because of their susceptibility of flow- induced shear degradation. Therefore, molecular degradation is one of the major defects in the drag reduction application, since the polymeric additives are exposed to strong turbulent elongation strain and shear stresses.

Polyethylene oxide (PEO) has been the most widely studied for both laboratory and commercial applications, including fire fighting and marine propulsion. (PEO) is a linear, flexible molecule which is available commercially in range of high molecular weights, its utility in multiple pass application is limited due to its extreme sensitivity to shear degradation. Drag reduction similar to that obtained in water has been shown for PEO in other solvents such as, sea water, plasma, benzene, dioxane, and chloroform. Mixed (PEO) system, such as (PEO) graft polymer, polymer / soap and polymer/dye mixture, has shown to provide varying levels of drag reduction effectiveness(18).

Polyacrylamide (PAAM) is the other synthetic water soluble that differs from PEO in that it has a side chain and is less susceptible to shear degradation (19). The related polymer poly (acrylic acid) (PAA) can be formed by hydrolysis of PAAM. Most of the laboratory and commercial studies, however, have focused on PEO and PAAM due to their availability, their relatively low cost, and the larger body of previously reported experiments describing their solution behavior available in the literature (19).

Modified cellulose compounds such as sodium carboxymethyl-cellulose (CMC) is available as drag-reducer agent in difference molecular weights. Xanthan Gum (XG) is another natural polymer which has been used as a commercial drag-reducer additive. XG is an intracellular polysaccharide produced by the bacteria Xanthomans. It shows greatest shear stability than for the flexible, long synthetic polymers (20).

A number of theories have appeared to explain how polymer molecules interfere with production, growth or transport of turbulent disturbances. The polymer hydrodynamic coil interacts with and disrupts the eddies and micro-vortices present in turbulent flows (21). At high strain rates, the polymer chain tends to elongate along the principal strain rate axis, and large extensions result. At the same time, a form of strain-rate hardening occurs in which the elongation viscosity becomes very high. As the elongation viscosity increases, the large scale bursts and sweeps in the wall layer flows are inhibited, thus reducing friction. Although many researchers feel that macromolecular extension is involved in turbulence suppression, there is still disagreement on this point. The many facets of Drag-reduction, e.g. the extremely dilute character of the polymer solutions, and the undefined nature of turbulent flow, make it a complex phenomenon to explain. Since Drag-reduction is characterized by large changes in the flow caused by the presence on a trace of additives, the objective of drag reduction studies is to seek an equally sensitive mechanism which can predict such a large effect at the dilutions involved.

2.2.2: Surfactant

Surfactants are surface active agents which are the main constituent in soaps and detergents, which also consist of a polar (hydrophilic) head and nonpolar (hydrophobic) tail. Depending on the electrical charge of the head group, the surfactants can be classified as anionic, cationic and nonionic. When the concentration of a surfactant solution exceeds a critical value, the surfactant molecules start to form aggregate, ie. micelles. The association of the molecules to micelles is reversible, ie. when the concentration is below the critical value the micelles will dissociate into molecules again (21).

Although the effect of surfactant solutions on Drag-reduction was conducted by Mysels as early as 1949. Surfactant additives have not been as exhaustive and have received less attention than polymer solutions. Ten years later more details were reviewed by the work of Dodge and Metzner (22), and Shaver and Merrill about the effectiveness of surfactants as drag-reducers(22) therefore surfactant solution as drag-reducers become a favorite drag reducer owing to their chemical and mechanical stability which is an important requirement for practical applications (22).

Following the pioneering work of Mysels (21) in non – aqueous systems, Savins carried out extensive work on anionic surfactants as drag reducers in aqueous solutions. Anionic surfactants are negatively charged, which allows them to interact with any positive ions present in solution, such as calcium and magnesium ions in tap water. Savins observed an interesting stress controlled DR effect in the soap solutions. The DR increased with increasing shear stress up to a critical value. Beyond the critical value, the DR of the soap solution became indistinguishable from that of the soap – free solution. This indicates that the network of micelles collapses if the shear stress exceeds critical shear stress. This occurs because of a temporary disentanglement of the network induced by turbulent vortices and eddies in fully developed flow (21). If the wall shear stress is reduced from above to below the critical value, then the Network bonds reform and the reducing ability of the solution is restored.

Mohammed studied the drag-reduction effectiveness of two anionic surfactants, Sodium Dodecyl Benzene (SDBS) and Sodium Lauryl Sulfate (SLES) in water circulation loop. She found that the SDBS detergent is more efficient than SLES additive due to the difference in their molecular structure (23).

Among the surfactants used for drag reduction, cationic types such as cethyltrimethylammonium chloride (CTAC) and Stearyltrimethylammoniym chloride (STAC) have been most widely used as additive. Sodium Salicylate is used usually as a counter-ion (24).

Cetryltrimethylammonium bromide (CTAB) is the cationic surfactant which has been investigated for drag reduction in detail. Gadd suggested the possibility of using the CTAB-naphthol mixture to reduce turbulent friction, because the mixture showed shear-thinning characteristics. Similar to anionic surfactant solutions, the drag reducing ability of the CTAB-naphthol solution terminated at some upper Reynolds number corresponding a critical shear stress where there was a scission of the micelles (25).

Elson et al. (15) (1983) used alkyl tri methyl ammonium halides with 1–naphthol as a drag reducing agent in aqueous solution to study the effect of solution concentration soap–naphthol ratio, soap molecular weight, and temperature of solution on drag reduction. The results showed that friction losses increases with increasing pipe diameter as show in Figure 2.1, also concluded that maximum drag reduction required low soap concentration.

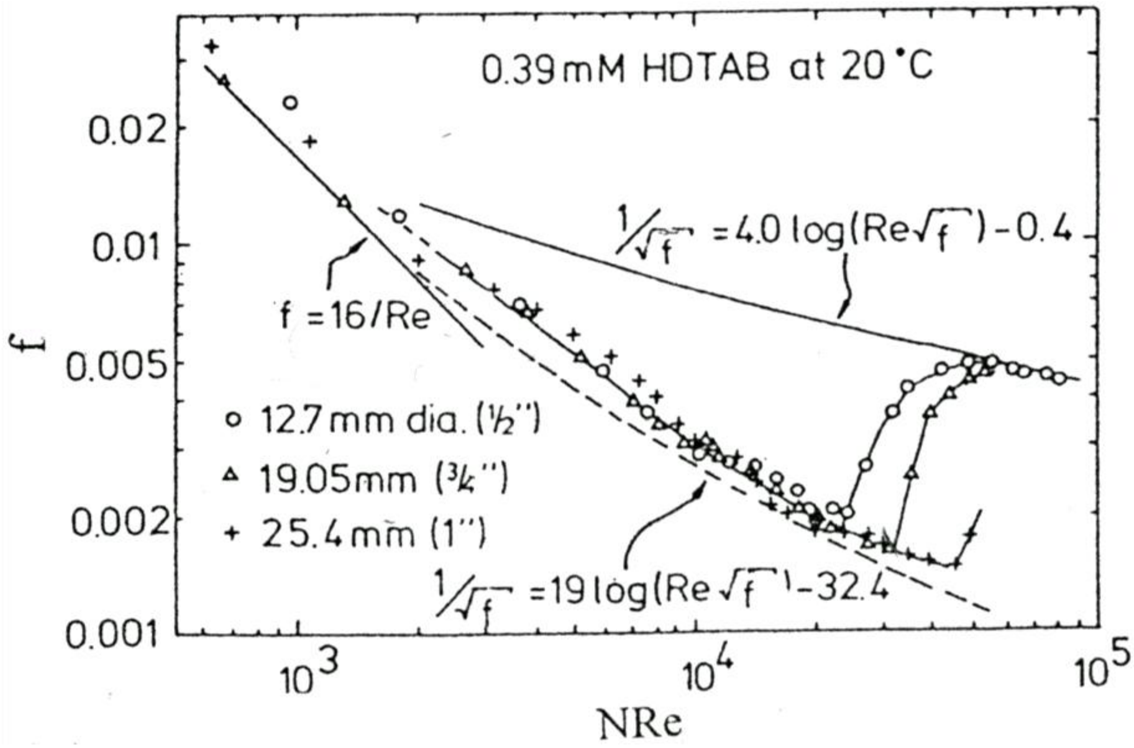

Figure 2.1, Effect of pipe diameter on friction factors of equimolar HDTAB, 1 – Naphthol solution (15)

Zakin et al. (26) (1993) used cationic Habon G surfactant (C16H33N(CH3)2C2H4OH)+ which consisted of 53.3% active surfactant, 10.2% iso propanol and 36.3% water flowing through section test of 4 cm. inside diameter pipe. The researchers concluded that surfactant solutions in water can reduce turbulent friction losses more than predicted by the Virk maximum drag reduction asymptote (MDRA). Elastic sub layer which means velocity profile in highly drag reducing surfactant solutions is steeper than that profile proposed by Virk as the (MDRA) for polymer solutions. Finally, Zakin et al. concluded that turbulence intensities for drag reducing surfactant systems are reduced from 20 to 35% of those for water at all locations in the tube.

Lin et.al (27) (2001) compared the effect of concentration of the counter ion and its ratio to surfactant concentration on drag reduction, Rheological behavior, and microstructures. They found Arquad 16-50 (commercial CTAC, cetyltrimethylammonium chloride) (5mM) with the counter-ion 3,4-dichlorobenzcate (5 and 10 mM), 3,4-dimethylbenzcate (5 and 10 mM) solutions are good drag reducers at different temperature ranges.

Katie and Zakin (28) (2005) studied number of Zwitterionic and cationic surfactants to determine the rheological properties of surfactant solutions and compare with their drag reducing properties. The rheological properties include shear viscosity, shear–induced structure and shear stress.

The studies on nonionic surfactants as drag reducers have been reported by Zakin and Chang (29, 30). They investigated the effect of temperature, electrolyte concentration, surfactant concentration and the effect of mechanical shear on three nonionic surfactants formed from linear alcohols and ethylene oxide moieties. They found that 1% solutions of the commercial surfactants like Alfonic 1214 were more effective than the 0.5 % solutions. The critical shear stress for mechanical degradation in the case of nonionic surfactant is dependent on the surfactant concentration, electrolyte type and concentration, and on the temperature. The molecular structure of the surfactant has an important effect on its micelle size and shape which in turn profoundly influence the drag reducing ability (29, 30).

Zakin (31) (1983) used large number of non–ionic surfactants to study the effect of surfactant structure, concentration, temperature and mechanical degradation on drag reduction. This was carried by using number of linear primary alcohol lethoxylate–surfactant in aqueous solution. The Brij 96 ($C_{18}H_{35}$–(OCH_2–CH_2)$_{10}$–OH) surfactant was more active than others. The used surfactant had the ability to self repair when it reaches a region of lower shear forces. Finally, showed that drag reduction increases with decreasing pipe diameter.

Surfactants solutions have become of favorite drag reducer owing to their chemical and mechanical stability that is an important requirement for practical applications. Development of surfactant systems exhibiting DR at concentration similar to dilute polymer solutions (< 100 ppm) have been disclosed in a number of recent patents (32).

When one compares the data for surfactant solutions with that for polymer solution, it becomes obvious that the drag reduction behaviors in these two cases are different. While the soap solution exhibits drag reduction at low wall shear stress values, the polymer solutions show relatively small drag reduction at low Reynolds numbers and increasingly large reduction at high Reynolds numbers. These two types of behavior are obviously a consequence of the morphological difference between micelle and polymeric structures (33). It can be assumed that:

1. The flexible polymer molecule needs to be elongated by a large velocity gradient before its full drag reducing ability is developed.
2. The surfactant particles are oriented much more easily at lower velocity gradients.

In terms of equivalent molecular weight, micelles are known to have larger values than polymers and therefore they would shift the onset of drag reduction to a lower shear stress value (33, 34).

2.2.3 Suspended particles

It is well known that the presence of suspended particles modifies the turbulent structure of the flow (35). The combination of general factors, such as sediment concentration, specific weight of solid and fluid, particle size and shape and others, can produce sub stationary changes in the behaviour of the flow. The most interesting case is that of a drag reduction which can occur in pipes when the combination of factors produces a decrease of turbulent intensity. The mechanisms which produce these changes in the turbulent structure could be various, depending upon the particle and flow characteristics and the overall effect could also vary for each particular case. Zaqustin (35) presented an analysis of a mechanism in which gravity is considered as the only factor involved in the turbulence. The same approach was obtained a few years later by Mahmood (36).

Clay solid particles were found to behave as efficient drag-reducing agent (DRA) (37). A gradual increase of drag-reduction and throughput was achieved by increasing the clay concentration and water flow rate and decreasing the pipe diameters. Moreover, the drag-reduction ability of carboxymethyl cellulose was improved noticeably by mixing with clay as combined additive (37).

Berge and Solsvik (38) (1996). Conducted different tests using both conventional gel-type DRA, and a new generation type additive. The new generation DRA was an emulsified powder product with a polymer content of about 20-25%. This new type turns out to be about four times efficient, in reducing drag, than conventional gel- type, DRA. They (38) also measured the drag efficiency as a function line fill and showed the relationship between injection rate of DRA and wax- deposits in a pipeline.

2.3 Microbubbles

Microbubble-modified boundary layer and associated skin friction reduction have been an active area of research for ship hull because of its energy saving potential (39). The DR in a turbulent boundary layer on a smooth wall can be realized by reducing the skin friction under suitable conditions when small gas bubbles are injected into the flow from an upstream position (39). The injection of gas into a liquid turbulent boundary layer to form bubbles reduces skin friction drag locally by as much as 80 %. Although it has long been know that a layer of air next to a surface in water reduces turbulent skin friction, the concept of the microbubble-modified boundary layer came into existence in its present form from the pioneering work of McCormick and Bhattacharyya (40). They used a copper wire wound around a towed body of revolution to produce hydrogen bubbles by electrolysis. Their experiments showed that microbubbles could reduce total drag and that the DR increased with increasing gas generation rate and decreasing rate. The results, however, were limited to Reynolds numbers between 0.3 and 1.8 million. Subsequently, several experiments conducted in the former Soviet Union reported significant drag reduction in water tunnel boundary layers by injection of air bubbles through flush-mounted porous plates (41, 42). In the 1980s, through a series of systematic studies in water tunnels the drag reducing effects on flat wall by microbubbles generated by porous plates (43, 44) and on axisymmetric body by circumferential porous rings (45, 46) were observed. Kato et al (47, 48) carried out several experiments with microbubbles in a flat plate boundary layer. In order to overcome the practical limitations of conventional porous plates, such as high injection energy and marine biofouling when used below a ship hull, a new injection method using a slit was devised (48).

Although the effectiveness of microbubbles has been demonstrated and the bubble sizes have been found to be one of the important factors affecting the DR, the overall mechanism that leads to this reduction is only poorly understood. In particular, the interaction between the bubbles and the boundary layer has not been studied extensively (49). Guin et al (50) investigated the DR effects due to the introduction of microbubbles into a two-dimensional water channel. The study established a relationship between the DR effectiveness and the near-wall bubble concentration. Pal et al (51) found that the bubbles were effective for drag reduction if they are located beyond a certain distance from the wall. The data of Guin et al (49) not only support their finding, but also provide some quantitative relation between drag reduction and near wall void fraction. Numerical investigations into the mechanisms of microbubble drag reduction have been conducted by Madavan et al (52). The action of the bubbles is simulated by allowing the viscosity and density to vary locally as a function of a prescribed bubble concentration profile. The results of the model show that substantial skin friction reductions can be obtained when microbubbles are present, thus supporting the idea that microbubbles can act not only as an agent to reduce skin friction, but also to reduce overall drag.

2.4 Compliant Coatings

2.4.1 Overview

Cetaceans seem to possess unusually low overall drag coefficients. Observation of the amazing swimming abilities of the dolphin led Kramer (53, 54) to design his first compliant coatings. He conducted his original experiments by towing a model behind an outboard motor boat. A typical successful coating giving at least 50 % drag-reduction, which consisted of a flexible inner skin, an outer diaphragm, and stubs, all made of soft natural rubber. The cavity between the outer diaphragm and the inner skin was usually filled with a highly viscous damping fluid. As his preliminary experiment indicated, the drag reduction was attributed to the delay of the transition of laminar-turbulent boundary layer to higher Reynolds number compared to that on a rigid wall.

After Kramer's original publications in 1957 and 1960 (53, 54), drag-reduction with compliant coatings has become a popular topic of research. Several investigations (55, 56) were conducted to duplicate Kramer's coating and his results, but no significant drag reduction was observed in any of these investigations. Since then, researchers have assumed that Kramer's results were in error and that his observations could have come about as a result of accidental excretion of the silicone oil used as the damping fluid during the tests. Although theoretical models have indicated that it is possible to stabilize a laminar boundary layer and to delay the transition of laminar-turbulent flows indefinitely with appropriate flexible materials. Experiments with compliant wall models in water and air flows have produced no conclusive data (48). During the 1970s various compliant materials were tested in water at the Naval Ocean Systems Center, the Naval Research Laboratory and the

Naval Undersea Warfare Center (57). In each case, no statistically significant reduction in drag was measured.

It was not until 1985 when careful analyses by Carpenter and Garrard (58) and well controlled experiments by Gaster (59) that, for the first time, provided direct confirmation of the transition delaying potential of compliant coatings. These vindicated Kramer’s original claims, and offered a plausible explanation for the failure of the subsequent laboratory experiments. It was shown that transition Reynolds numbers, which exceed by an order of magnitude those on rigid surface boundary layers, can be achieved.

2.4.2 Coating Optimization

The following considerations should be made, if a compliant coating is to be designed for use on a vehicle (60).

(1) What limits the transition-delaying performance of a compliant wall?
(2) What is greatest possible transition delay achievable?
(3) What are the optimum wall properties to give the greatest transition delay?

These questions have been addressed (61, 62) for the plate-spring compliant wall originally introduced by Carpenter and Garrard (58) as a theoretical model of the Kramer coating. In the past, there was a rule of thumb: “If it is soft, let us try it” (57). A wall that is too compliant (ie. too soft) can substantially delay transition, but rapid breakdown can occur through the amplification of wall based instabilities. Figure 2.2 shows different types of compliant wall which comprises a soft viscoelastic substrate surmounted by a thin, much stiffer outer layer (60). Such walls are simpler to manufacture and are regarded as more practical. Carpenter (62) suggested that a multiple-panel coating, placed in series, with each panel optimized for a particular range of Reynolds numbers, is likely to produce larger transition delays than a single-panel coating.

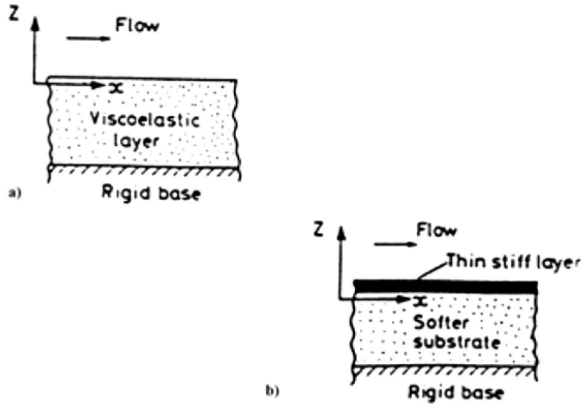

Figure 2.2, Schematic of the compliant wall, (a) Single layer and (b) Double layer (52).

Chung (63) devised a composite compliant coating that can reduce the skin friction on a rotating disc up to 21% at the Reynolds number of $8.92*10^5$. The coating was fabricated out of four major components as shown in figure 2.3, (1) a thin stiff film as the top layer, (2) a low modulus high damping silicone elastomer as a thin layer embedded on (3) the rayon fabric, and (4) a support screen. The stiffness of the top film greatly influenced the performance of the coating. The use of a Teflon film (0.13 mm thick) led to the best result for Chung's work in the Reynolds number range of $8.92 * 10^5$ to $1.94 * 10^6$. Chung (63) postulated that the top film helps reduce skin-friction due to (1) top film stabilizes the compliant surface from forming static divergence which increases skinfriction drastically, and (2) the high modulus film may be resonant to the turbulent fluctuations at high frequencies which helps the coating to reduce the skin-friction in the turbulent boundary layer. Chung concluded that high loss tangent reduces the skin-friction more effectively than a low damping coating.

Many theoretical studies have shown that the turbulent-laminar transition can be delayed through the attenuation of so called “Tollmien-Schlichting waves” (TSW) (64) .The early work of Benjamin (64) and Landahl (65) showed that as the compliance characteristics of a coating is increases the growth of the TSW is progressively suppressed. Theoretically, if the coating were to be made sufficiently compliant the TSW would be completely stabilized resulting in the maintenance of laminar flow for indefinitely high Reynolds numbers. Optimization of viscoelastic compliant coatings has been theoretically examined by Dixon et al (60). These authors determined the best transition-delaying performance possible using compliant coatings made from viscoelastic materials.

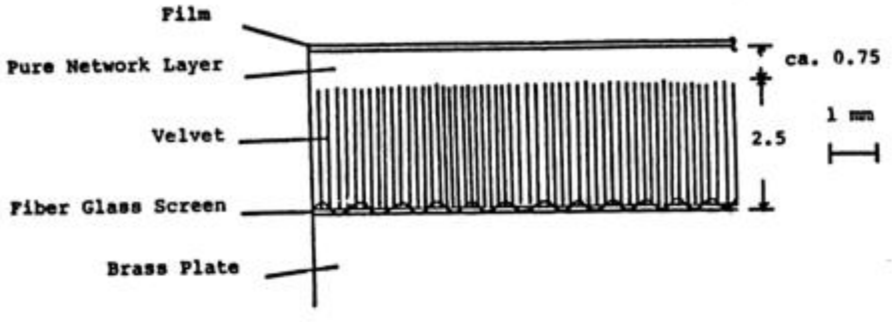

Figure 2.3, Detail of compliant coating (48)

2.5. Hypothetical Mechanism

Hypothesis of drag reduction mechanism is explained on the basis of figure 2.4. The polymer–surfactant structure before flowing is presented in figure. 2.4.1. Polymer film is forming around a micelle. That structure is a general accepted model explaining effect of interaction between polymer and surfactant. On a base of that model, experimental results can be interpreted in a simple way (66). Figures, 2.4.2–2.4.5, represent the structures corresponding to flow ranges numbered 2–5 in figure 2.4 In a pipe flow, aggregates take preferred orientation according to minimum resistance principle as show in figure 2.4.2. When the Reynolds number increases, the aggregates elongate(67). They are responsible for drag reduction inside liquid. When Reynolds number reaches critical point, drag reduction of surfactant solution alone disappears, while that of polymer–micellar solution still exists. Aggregates probably disintegrate as show in figure 2.4.3.

Polymer macromolecules and micelles start to influence the solution individually. The transition zone between laminar and turbulent flow is extended towards larger Reynolds numbers. Afterwards, critical Reynolds number for polymer–micellar solution appears. Micelles lose their orientation. Polymer macromolecules assume a small coil shape figure 2.4.4. Increasing shear rate causes extension of macromolecules along flow direction. They damp dissipative eddies in turbulent zone. This is the reason why micelles recover ordered orientation according to minimum resistance principle as show in figure 2.4.5. All those structures are responsible for drag reduction. Hypothetical structures presented in figures. 2.4.2–2.4.5 in a good way explains flow ranges appeared on the curve of friction behaviour.

at study state

at laminar flow rate

at transition region

between laminar

and turbulent.

at turbulent flow

rate

at high Reynold's

No.

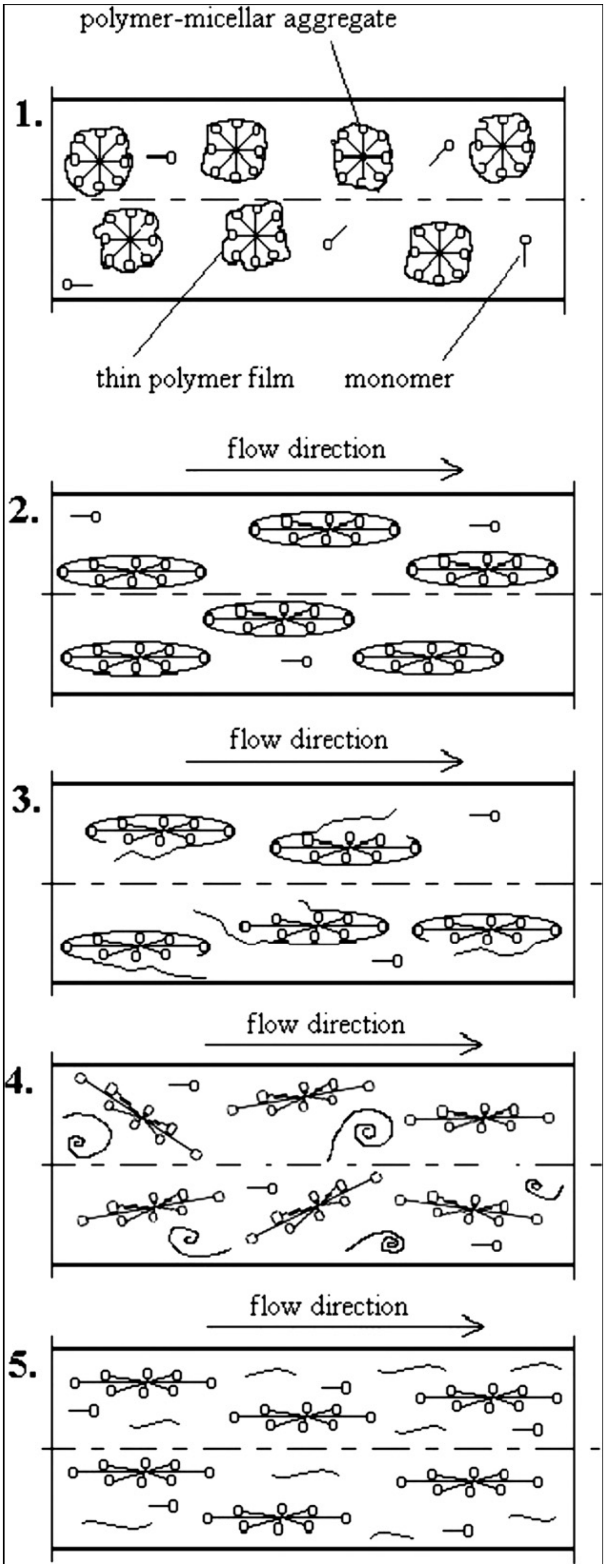

Fig. 2.4 Hypothetical mechanism of drag reduction

2.6. Friction

2.6.1 Fundamentals

When a fluid with uniform flow over the cross-section enters a pipe, the layers of fluid adjacent to the walls are slowed down as on a plane surface and boundary layer forms at the entrance. This build up in thickness as the fluid passes in to the pipe. At the some distance down stream from mouth, the boundary layers reach a thickness equal to the pipe radius and join at the axis, after which condition remain constant and fully developed flow exists. If the flow in the boundary layers is streamline when they meet, laminar flow exists in the pipe. If the transition has already taken place before the meet, turbulent flow will persist in the region of fully developed flow (68, 69).

Stanton and panel 1945(70) measured the drop in the pressure due to friction for a number of fluid flowing in pipes of various diameter and surface roughness. They expressed their results by using the concept of a friction factor, defined as the dimension less group $R/\rho u^2$, which is plotted as a function of Reynolds number as shown in figure 2.5. ($R= -R_0$) represent resistance to flow per unit area of pipe surface. For a given surface a single curve was found to express the results for all fluids, pipe diameter, and velocities.

At low values of Reynolds number ($Re< 2000$), $R/\rho u^2$ was independent of the roughness, but at high values ($Re>2500$), $R/\rho u^2$ varied with the surface roughness, while at very high Reynolds number the friction factor (f) became independent of Re and it is a function of the surface roughness only. Over the transition region of Re, from 2000 to 2500 $R/\rho u^2$, increase very rapidly. Showing the great increasing in friction as soon as turbulent motion commenced. This problem associated with fluid motion, heat transfer, and mass transfer. Mody 1944 (71) worked in terms of a friction factor (here denoted by $f^{\backslash}$) equal to $8R/\rho u^2$ and expressed this factor as a functional of two dimension less terms Re and e/d where e is the length representing the magnitude of the surface roughness. These relationships can be seen from dimensional analysis.

The effect of chemical additives on solvent structure may be as important as the effect of solution on additive conformation in drag-reducing solution especially if the solvent is water. Water is a highly ordered liquid due to its polar nature and its propensity to form hydrogen bonds between molecules. The hydrogen bonds are constantly breaking and reforming, producing transient clusters involving different molecules throughout the fluid. McCormick (72) and Morgan (73) have indicated that structure may be of great importance in the drag reduction phenomenon. They measured the friction factor for a solution of hydrophobically modified acryl amid copolymer (PAAM-35) in which polymer concentration has been held constant but solvent has been varied. Solvent employed were dionized.

Figure 2.5 represents a pipe friction chart φ versus Reynolds Number, where R is a function of U, d, ρ, μ and e. the analysis gives (68).

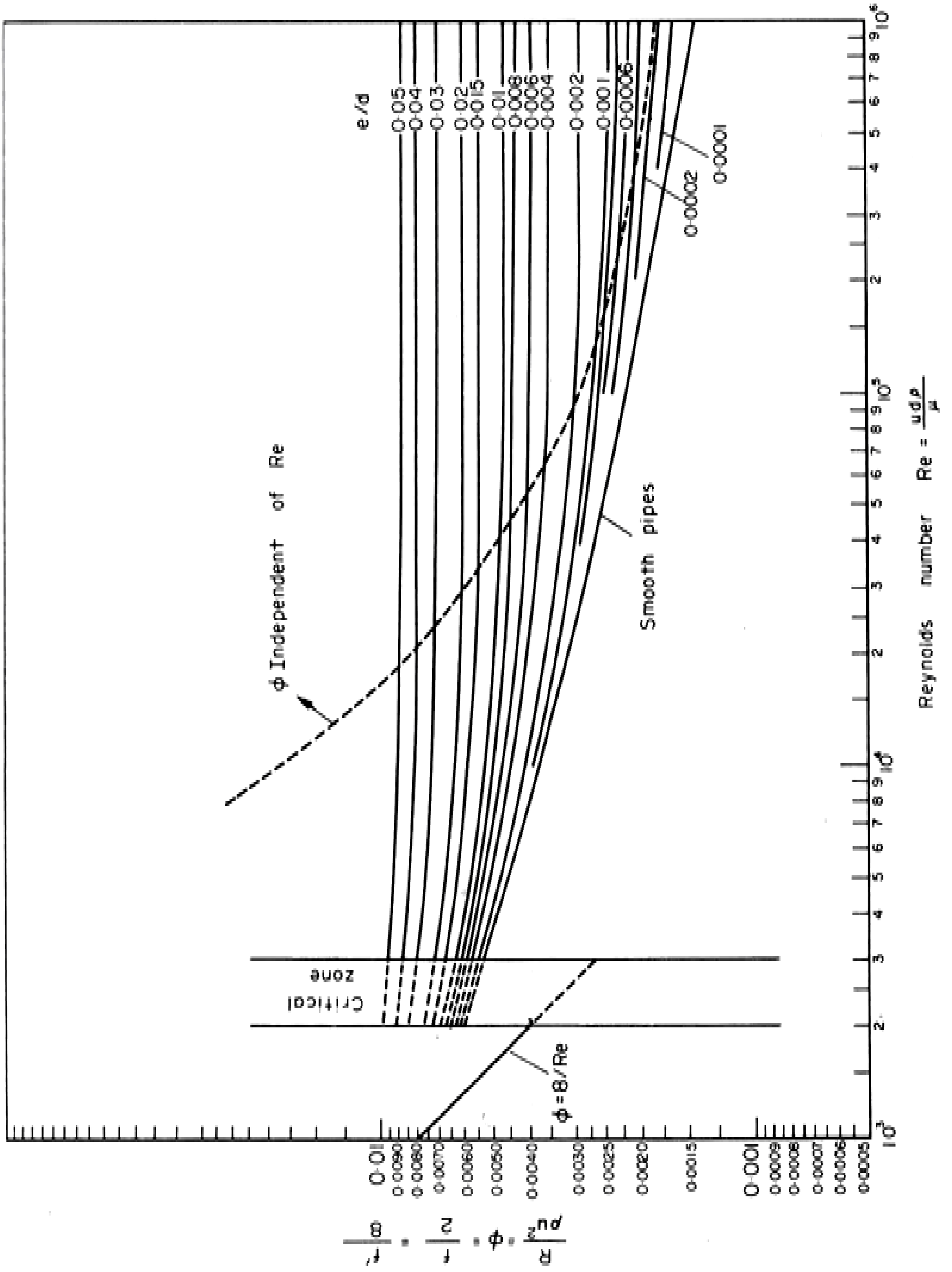

Figure 2.5, Pipe friction chart φ verses Re. (68)

$$\frac{R}{\rho u^2} = \text{function of } \left(\frac{u\,d\,\rho}{\mu}\right) \text{ and } \left(\frac{e}{d}\right) \qquad \text{... (2.1)}$$

Thus a single curve will correlated the friction factor with the Reynolds number or group for all pipes with the same degree of roughness of e/d. This curve is of very great importance since it not only determines the pressure loss in the flow but can often be related to heat transfer or mass transfer.

Such a series of curves for varying values of e/d is given in figure 2.5 which shows the values of $R/\rho u^2$ and the values of the moody factor f related to Reynolds group. Four separate regions can be distinguished:

Region 1: (Re <2000) corresponds to streamline motion and a single curve represent all the data, irrespective of the roughness of the pipe surface. The equation of the curve is: (68).

$$\frac{R}{\rho u^2} = \varphi = \frac{\acute{f}}{8} = \frac{f}{2} = \frac{8}{Re} \qquad \text{... (2.2)}$$

$$f = \frac{16}{Re} \qquad \text{… (2.3)}$$

Region 2: (2000<Re <3000) is a transition region between streamline and turbulent flow conditions. Reproducible value of pressure drop cannot be obtained in this region, but the value of $R/\rho u^2 = f/2$ is considerably higher than in the streamline region. If an unstable form of streamline flow does persist at Re greater than 2000, the friction force will correspond to that given by the curve $R/\rho u^2 = 8/Re$, extrapolated to values of Re greater than 2000. (68)

Region 3: (Re > 3000) correspond to turbulent region of the fluid and $R/\rho u^2$ is a function of both Re and e/d with rough pipe giving high values of

$R/\rho u^2$. For smooth pipe there is a lower limit which $R/\rho u^2$, does not fall for any particular value of Re.

Region 4: Rough pipes at high Re. In this region the friction factor becomes independent of Re and depends only on $(\frac{e}{d})$ as shown below: (74)

$\frac{e}{d} = 0.05$ $Re>1*10^5$ $R/\rho u^2 = 0.087$ ... (2.4)

$\frac{e}{d} = 0.0075$ $Re>1*10^5$ $R/\rho u^2 = 0.0042$ ... (2.5)

$\frac{e}{d} = 0.001$ $Re>1*10^5$ $R/\rho u^2 = 0.0024$ ... (2.6)

A number of expressions have been proposed for calculating R/ρu2 =φ in terms of Reynolds number and some of these are given below (74).

Smooth pipes:

$2.5*10^3 < Re < 10^5$ $\varphi = 0.0396\, Re^{-0.25}$ ... (2.7)

Smooth pipes:

$2.5*10^3 < Re < 10^7$ $\varphi^{-0.5} = 2.5 \ln (Re\, \varphi^{0.5}) + 0.3$ ... (2.8)

Rough pipe:

$\Phi^{-0.5} = 2.5\ln (0.27\frac{e}{d}) + 0.885Re^{-1}\, \varphi^{-0.5}$ ... (2.9)

Rough pipe:

$(\frac{e}{d})$ Re φ0.5>>3.2 $\varphi^{-0.5} = 3.2 - 2.5\ln (\frac{e}{d})$ ... (2.10)

Equation 2.7 is due to (Blasius) (75) and the others are derived from considerations of velocity profile. In addition to the moody friction factor

$f^{\backslash} = 8\frac{R}{\rho u^2}$, the fanning or Darcy friction factor $f = 2\frac{R}{\rho u^2}$ is often used in American texts. It is extremely important therefore to ensure that the precise meaning of the friction factor is clear when using this term in calculating head losses due to friction (68).

The head loss due to friction is expressed by Darcy's equation as follows:-

$$h_f = 8\varphi\left(\frac{L}{2d}\right)\left(\frac{u^2}{g}\right) \qquad \text{... (2.11)}$$

$$h_f = 4\varphi\left(\frac{L}{2d}\right)\left(\frac{u^2}{g}\right), \varphi = f \qquad \text{... (2.12)}$$

and $h_f = 4f\left(\frac{L}{2d}\right)\left(\frac{u^2}{g}\right)$ … (2.13)

and in more conventional pipeline unites, is expressed in term of pressure drop:

$$\Delta p = 4f.\left(\frac{L}{2d}\right).\rho u^2 \qquad \text{... (2.14)}$$

and $f = (\frac{\Delta p.d}{2L\,\rho u^2})$ ... (2.15)

For turbulent flow and smooth pipe,

$$f = \frac{0.04}{Re^{0.25}} \qquad \text{... (2.16)}$$

Where the Reynolds number:

$$Re = \frac{\rho u d}{\mu} \qquad \text{... (2.17)}$$

Equation (2.17) can be written by considering (2.14) and (2.15) as follows:

$$\frac{\Delta p}{L} = \frac{0.08\,\rho^{0.75}.u^{1.75}.\mu^{0.25}}{d^{1.25}} \qquad \text{... (2.18)}$$

The liquid velocity is calculated by equation (2.19).

$$U = \frac{Q}{A} = \frac{Q}{(\frac{\pi}{4})d^2} = 1.27 * (\frac{Q}{d^2}) \qquad \text{... (2.19)}$$

Therefore, the pressure drop is estimated by:

$$\frac{\Delta p}{L} = \frac{0.244\ Q^{1.75}.\mu^{0.25}.\rho^{0.75}}{d^{4.75}} \qquad \text{... (2.20)}$$

The power required for pumping will be given by the product of the volumetric flow rate and the pressure difference between the pump and the discharge of the pipeline,

$$H_p = \Delta p.(\frac{Q}{\eta_p}) \qquad \text{... (2.21)}$$

The required pump power is calculated by assuming constant flow rate, as follows:

$$H_p = (\frac{0.244\ Q^{2.75}}{d^{4.75}\eta_p}).\rho^{0.75}\ \mu^{0.25} \qquad \text{... (2.22)}$$

While, the volumetric flow rate is calculated by constant pumping horse power as follows:

$$Q = (\frac{d^{4.75}\eta_p H_p}{0.24\mu^{0.25}\rho^{0.75}L})^{-0.03637} \qquad \text{... (2.23)}$$

2.6.2 Friction Factor

Friction factor (also called flow improver) have involved from original ″gel_like″ products to suspension products. Flow improvers were initially limited to conventional applications in the pipeline industry (42).

The phenomena of friction and drag reduction was first observed more than 60 years ago, it was not until (1979) that friction reduction technology was developed enough to be used on a commercial scale on the Trans_Alaska pipeline. Initially, the pipeline industry believed only in conventional the industry about the capabilities of flow improvers (42).

In the process of transferring a Newtonian fluid through a pipeline system, considerable energy may be expanded to over come friction encountered in moment of the liquid. When a liquid is pumped under pressure frictional pressure is apparent as a pressure drop along the pipeline (42).

The fluid flow through pipes is subjected to resistance due to viscosity, fluid turbulence and roughness of the pipe surface. In order to overcome these resistances, the flow has to expand its energy and consequently, the available energy decrease in the direction of flow resulting in a downward sloping energy line (42).

The basic friction factor in pipe flow can be written in term of fanning friction factor as: (76)

$$f = \frac{\Delta P . D / 4L}{\rho v^2 / 2} \qquad \dots (2.24)$$

According to Reynolds number and properties of the system, some relationships of the friction factor declared by some authors.

For Re < 2100, Poiseuille,s law (77) is applicable.

$$f = \frac{16}{\mathrm{Re}} \qquad \dots (2.3)$$

For Reynolds numbers between 2100 and 4000 Wilson and Azad (78) derived an empirical equation for the central portion of the transition regime.

$$f = 7.1 * 10^{-10} * \mathrm{Re}^{2} \qquad \dots (2.25)$$

For Reynolds numbers up to 100.000 and smooth cylindrical pipes, Blasius (81) found that the friction factor can be expressed as follow:

$$f = \frac{0.079}{Re^{0.25}} \qquad \dots (2.26)$$

Von Karman (75, 79), found an alternative to Blasius equation for the turbulent flow of Newtonian fluids in smooth cylindrical pipes which can be written as follow:

$$\frac{1}{\sqrt{f}} = 4 \log\left(Re\, f^{1/2}\right) - 0.4 \qquad \dots (2.27)$$

Virk (76), represent the greatest possible fall in resistance in which the relation between friction factor (f) and Re does not depend on the nature of the additives or pipe diameter. The formula for Virk is:

$$f = 0.59 Re^{-0.58} \qquad \dots (2.28)$$

Nikuradse (78) determined asymptotic expression for fully developed turbulent flow in rough pipe as follows:

$$\frac{1}{\sqrt{f}} = 1.737 \ln(3.707 \frac{D}{\varepsilon}) \qquad \dots (2.29)$$

CHAPTR THREE

EXPERIMENTER WORK

3.1 Materials

The additives used in the present work were polyethylene Oxide (PEO), Polyacrylamide (PAAM), Xanthan Gum (XG) as water soluble polymers, Clay, and Alum as suspended particles. Furthermore, the water soluble Trisodium Polyphosphate (STPP), which is used usually as a builder in detergent compounding to eliminate the effect of water hardness, was considered also as drag-reducing agent for first time in the present work.

PEO of seven millions g/mole molecular weight was acquired from Sigma - Aldrich Company for Chemical Compounds, Linear formula $(CH_2CH_2O\text{-})_n$. PAAM with a molecular weight of $3.7*10^6$g/mole was supplied from DOW Chemicals Company, linear formula $(\text{-}CH_2CHCONH_2\text{-})$. While XG of $4*10^6$ g/mole molecular weight, chemical formula $((C_{35}H_{49}O_{29})_n$), was supplied by the general company of Vegetable Oil Industries, Baghdad. General formula of STPP $(Na_5P_3O_{10})$ and the molecular weight 367.86 g/mole. Clay of a high purity (Kaolin), chemical formula $(Al_2Si_2O_5(OH)_4)$, and Aluminum sulfate (Alum) were brought form local market. Alum $(KAl(SO_4)_2.12H_2O)$ is used usually for water treatment to remove suspended slurries. Tap water was used as flowing fluid.

3.2 Preparation of additives solutions

The method of dissolving of polymeric and STPP additives adapted here was to make 2% by weight additive solution in separate container. Therefore about 14 g of additive was mixed with 750 ml of water.

The solution will be stirred by a shaker for 1 hour for the STPP and about 30 hours for PEO, PAAM, and XG. The solution allowed to standing for 24 hours at room temperature prior to its uses and then carefully transferred to the test apparatus. Care should be taken also to avoid degradation of polymer during mixing and transfer.

The Shaker was used to avoid additive molecular degradation because the Shaker has no blade or sharp edge that could expose the additive to high shear force. Type of Shaker was KOTTGRMANN 4019 GGPMAMY, of 100 rpm as show in figure 3.1.

The clay has been crushed carefully by a hammer and the required amount of Clay and Alum were suspended in 750 ml of water.

Figure 3.1, Shaker

3.3 Flow Loop

A laboratory circulation loop system consists of a reservoir tank, gear pump, flow meter, manometer, pipes and valves; Izzat N. Slaiman(84) was used to perform the experiments, as shown in figure 3.2.

The reservoir tank of 0.49 m^3 capacity was supported by a galvanized pipe 31.75 mm (1.25 inch) inside diameter. A gear pump of 50.8 mm diameter and 1440 rpm was used to deliver the fluid to the testing sections.

Piping starts from the reservoir tank through the pump, reaching a connection that splits the pipe into two sections. The first section returns back to the tank using a 50.8 mm pipe as by pass and the other splits into three sections with 12.7, 31.75, and 50.8 mm pipe diameters (test section).

The test section of 2 m long was placed away from the entrance length. The minimum entrance length required for a fully developed flow profile in turbulent flow was calculated from the relationship suggested by Desissler, as given in equation 3.1 (80).

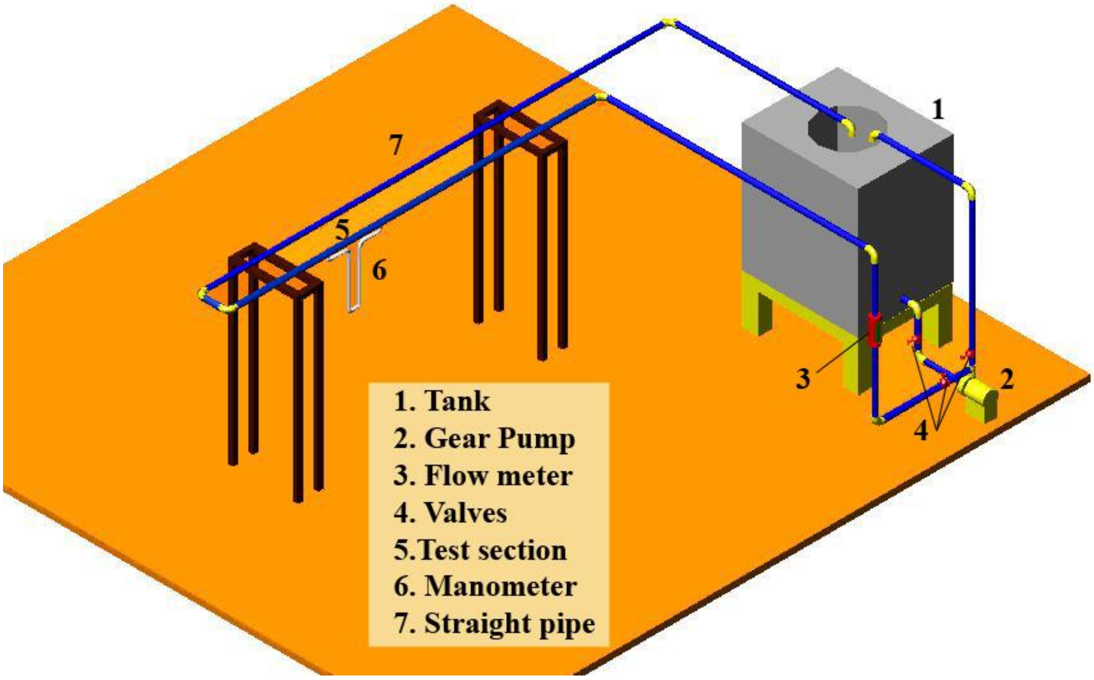

Figure 3.2, Schematic diagram of experimental rig

$$Le = 50\,D \qquad \ldots (3.1)$$

There,

Le = entrance length, m

D = pipe diameter, m

Therefore, the minimum entrance length for the used pipe of 1.25 inch inside diameter is,

$Le = 50 * 0.03175 = 1.5875$ m

The water flow rate was measured with a float flow meter, of 50.8 mm diameter and flow indicating range between 0.5 – 6.0 m^3/h. Figure 3.3, shows the calibration of the flow meter.

A U-tube manometer was used to evaluate the pressure measurements in mmH_2O.

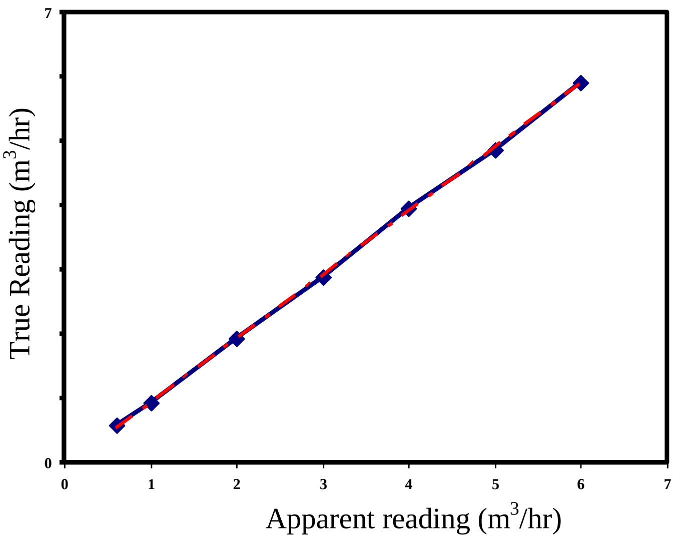

Figure3.3, Calibration of flow meter

3.4 Experimental Procedure

The experiments were started by cleaning the rig by tap water in the reservoir tank and circulated it in the piping system about 20 min and then discharged out side the flow system. The cleaned reservoir tank was filled initially about 140 liters Tap-water. The addition of additive was taken in weight part per million (ppm) which was mixed with about one liter, water and mixed by hand-shaking and then poured in the solution reservoir tank. The solution was allowed to flow through the pipe by operating the gear pump, and about 30 minutes of mixing was allowed prior to performing the test.

Connect each tube end of the pressure taps in the upstream and down stream with U-tube manometer , and allow the bubbles in the connecting Vinyl tubes to flow away , to avoid any error by reading . When the level of the water in manometer is in one level that indicate the reading of manometer is right. The solution flow rate was maintaining constant by means the corresponding valves. The experiment was stopped after obtaining a stabilized pressure drop reading.

3.5 Calculations

The weight of polymer required to prepare (x) ppm in 140 liter of water is obtained from the following equation:

$$grams = \frac{\rho_{water} * 140 * x}{10^6} \qquad \text{… (3.2)}$$

For example to obtain 50 ppm:

$$\text{grams} = \frac{1000 * 140 * 50}{10^6} = 7 \quad \text{g polymer}$$

For 2% polymer solution

$$= \frac{7 * 100}{2} = 350 \text{ g solution}$$

Percentage drag reduction, %DR is calculated by using pressure drop measurements in the test section for untreated ΔP and with polymer treated water, ΔPs (81), as follows

$$\%D.R = \frac{\Delta P - \Delta P_s}{\Delta P} * 100 \qquad \text{… (3.3)}$$

Fanning friction factor was calculated by using the following equation (82).

$$f = \frac{\Delta P . D / 4L}{\rho . U^2 / 2} \qquad \text{… (3.4)}$$

CHAPTER FOUR

RESULTS AND DISCUSSION

4.1 Introduction

Introduction screening study was designed to evaluate and compare the drag-reduction effectiveness of three different types' additives, polymers, STPP, and fine particles. The polymers are two water soluble flexible synthetic types, namely polyethylene oxide (PEO) and Polyacrylamide (PAAM), and Xanthan Gum (XG) as rigid polymers from natural resources.

Trisodium Polyphosphate (STPP) additive was considered in the present investigation for the first time as drag-reducing agent. While, Clay and Aluminum sulfate (Alum) were used as fine suspended particle agents.

Furthermore, mixtures of two types of the considered additives were used to investigate the performance of drag-reduction and to show a possible enhancement of drag-reduction effectiveness of individual additives.

A fully developed turbulent flow was considered through a straight pipe with inside diameter of 1.25 inch (0.03175 m) at temperatures within 18-25 ºC.

The effect of additive concentration and degree of turbulence was investigated in a laboratory circulation loop using tap water. Since turbulent flow is necessary for drag-reduction to occur, the system was operated for Reynolds number ranging 22278.9- 66836.7, which produced by a positive displacement gear pump to avoid any mechanical degradation of polymeric chains.

The experimental work was evaluated by measuring pressure drop for treated flowing water. The results are presented as percentage drag-reduction and friction factor, illustrated in figures and discussed in details. All experimental data are reported in Appendices A and B.

The calibration of flowing system was done with untreated tap-water prior to testing the experiments. Figure 4.1 shows the pressure drops date for the 1.25 inch (0.03175 m) pipe diameter used at laboratory temperature.

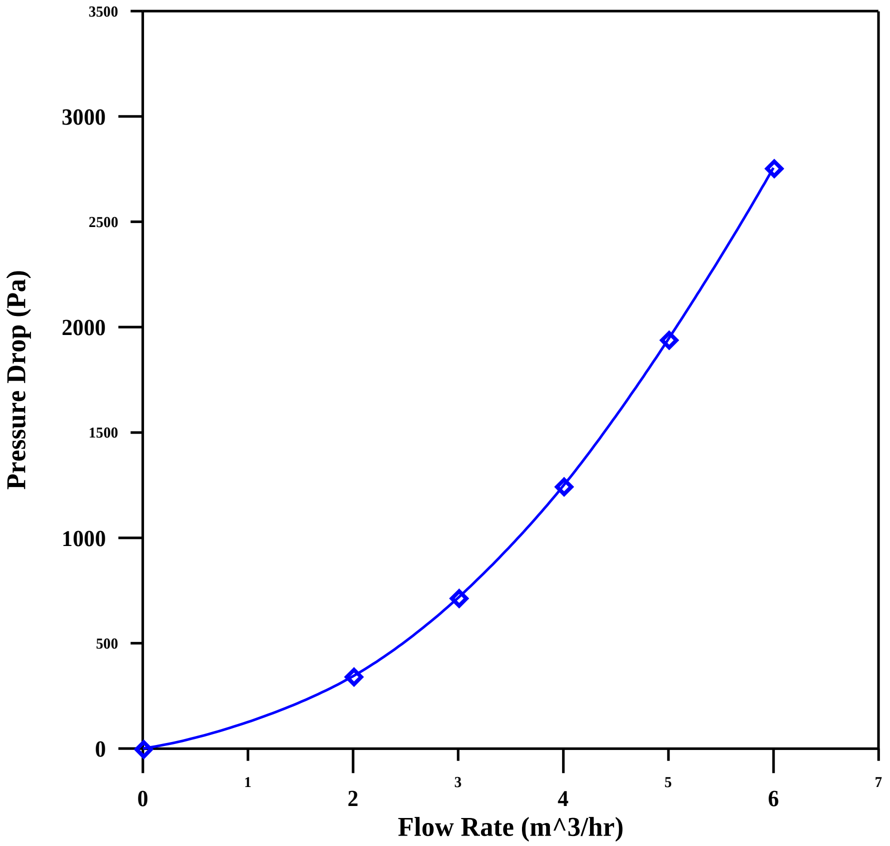

Figure 4.1, pressure drop vs. flow rate of for untreated water

As illustrated in figure 4.1, gradual increase of pressure drop is observed with increasing the bulk velocity.

4.2 Polymeric Additives

4.2.1 Concentration Effect

The effect of additive concentration was investigated over a range of 10 to 100 ppm for Polyethylene oxide and Polyacrylamide and 50 to 200 ppm for Xanthan Gum as drag-reducing agent. This might have been economically feasible for commercial applications. Furthermore, within concentrations used, Newtonian behavior was observed for all polymer solutions.

Figures 4.2, 4.3, and 4.4 summarize the concentration effect of PEO, PAAM, and XG agent on percentage drag-reduction of turbulent water flow respectively. A gradual increase of drag- reduction was observed with increasing the additive concentration for all considered polymeric additives. Since the polymer induced turbulent drag reduction is induced by the viscoelastic behavior contributions from the individual polymer molecules, and they may cause an interaction with turbulent eddies.

Consequently, a remarkable drag-reduction is observed with increasing the concentration (85).

Furthermore, the efficiency of long flexible polymers, polyethylene oxide and polyacrylamide is noticeable highs than for the rigid polysaccharide Xanthan Gum additives. The data for 6 m^3/hr flow rate indicate that about 8.5% and 11.5 % drag reduction were achieved by addition of 10 ppm PEO and PAAM respectively. While about 31.4% and 31.7% were obtained for 100 ppm additive as shown in figures 4.2, and 4.3 respectively. The values are about 7% and 16.2% by addition of 50 and 200 ppm XG, as show in figure 4.4.

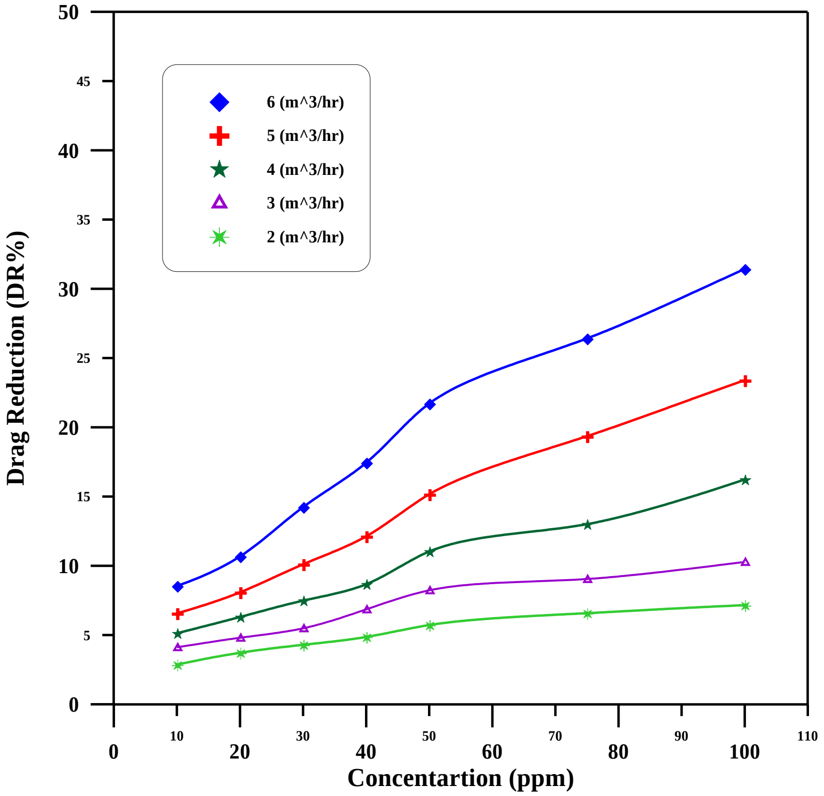

Figure 4.2, Percent drag-reduction vs. concentrations for different flow rates for Polyethylene Oxide PEO.

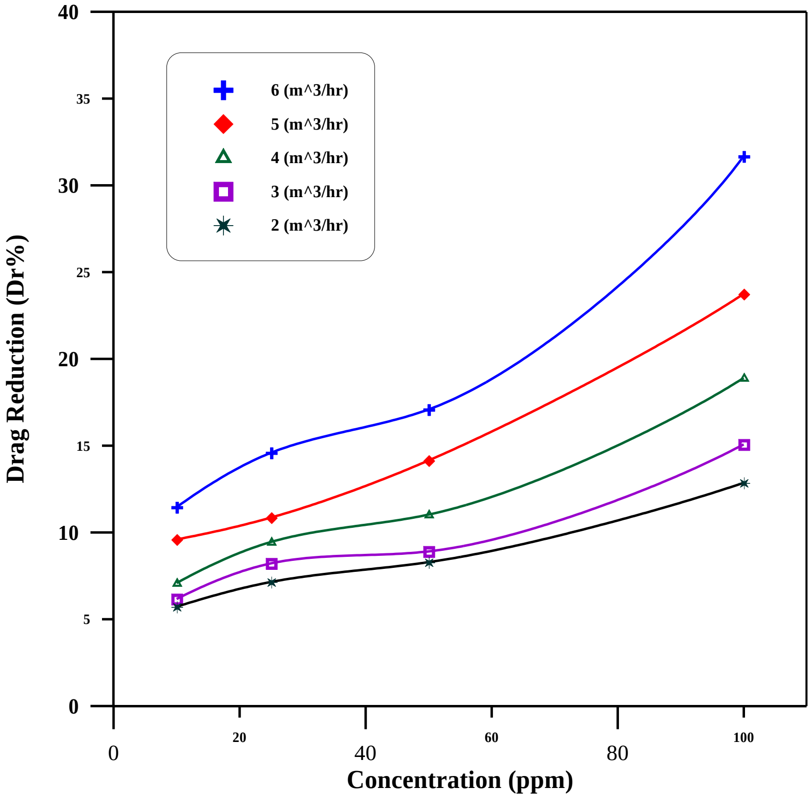

Figure 4.3, Percent drag-reduction vs. concentrations for different flow rates for polyacrylamide (PAAM).

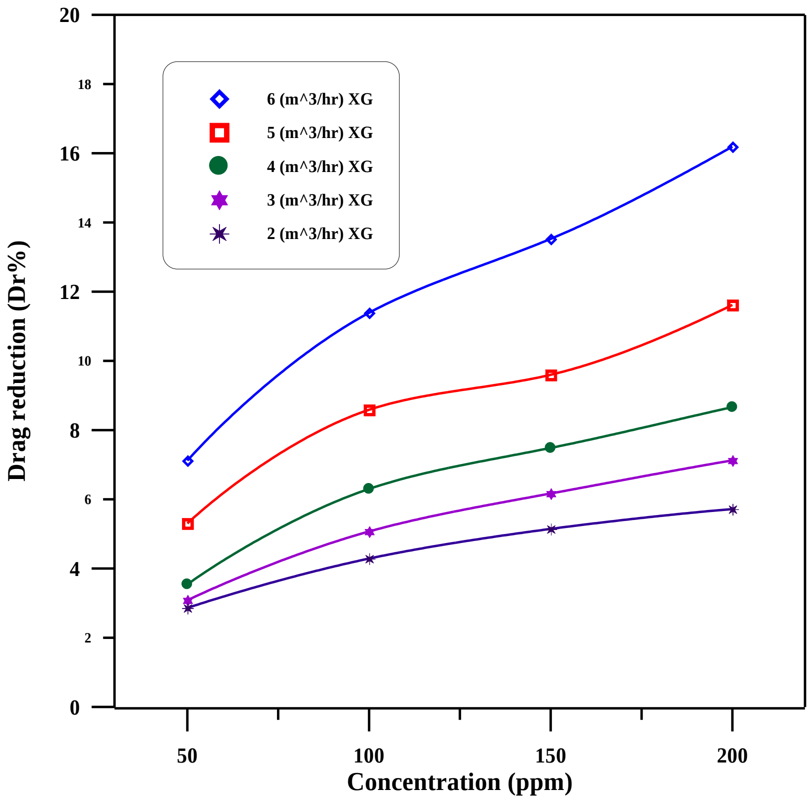

Figure 4.4, Percent drag-reduction vs. concentrations for different flow rates for Xanthan Gum (XG).

4.2.2 Flow Rate Effect

Since turbulent flow is necessary for drag-reduction to occur, different flow rates were chosen to study the effect of turbulency on drag-reduction effectiveness of polymeric additives. Therefore the performance of PEO, PAAM and XG additives was conducted for five different volumetric flow rates, 2, 3, 4, 5 and 6m^3/h, as illustrated in figures 4.5, 4.6, and 4.7 respectively. The results indicate that increase of flow rate perform the effectiveness of such polymeric additive noticeable.

The variation of drag-reduction with the solution flow rate agrees with Berman (86) in which reported that an increase in the Reynolds number leads to an increase in the strain rate and decrease in the time scale. Then the elongation reaches a constant level for a given solution and pipe diameter when no other limits are present.

Above 100 % increase in percentage drag-reduction is observed when the solvent flow rate increases from 3.0m^3/hr to 6.0m^3/hr at 100 ppm polymeric additive, as shown in figures 4.5, 4.6, and 4.7. This observation supports the predominate effect of turbulency on effectiveness of such drag-reducer agents (85).

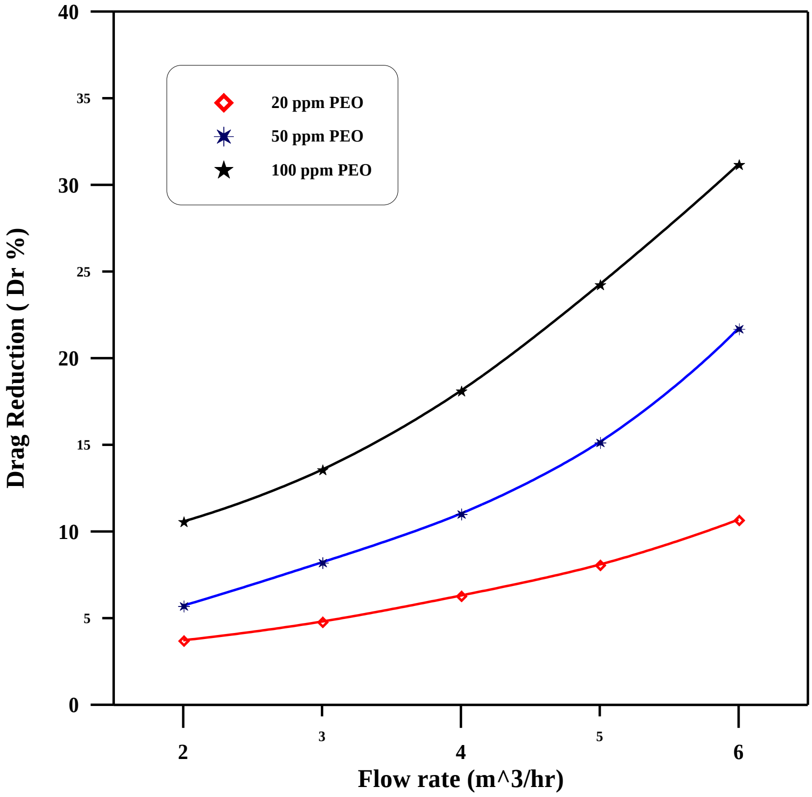

Figure 4.5, Percent drag reduction vs. flow rate for three selected concentrations of Polyethylene Oxide (PEO)

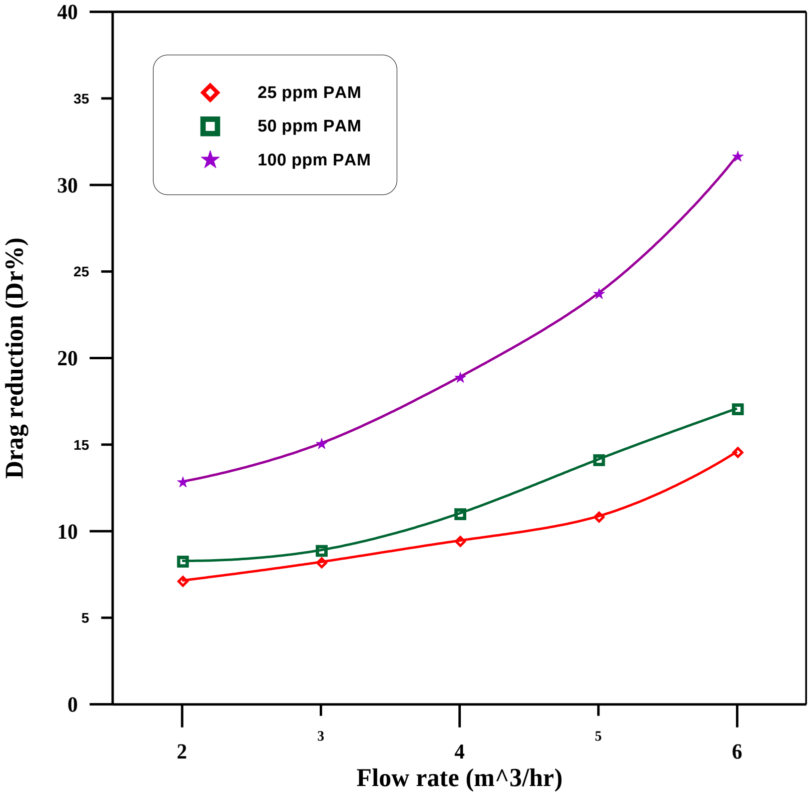

Figure 4.6, Percent drag reduction vs. flow rate for three selected concentrations of polyacrylamide (PAAM).

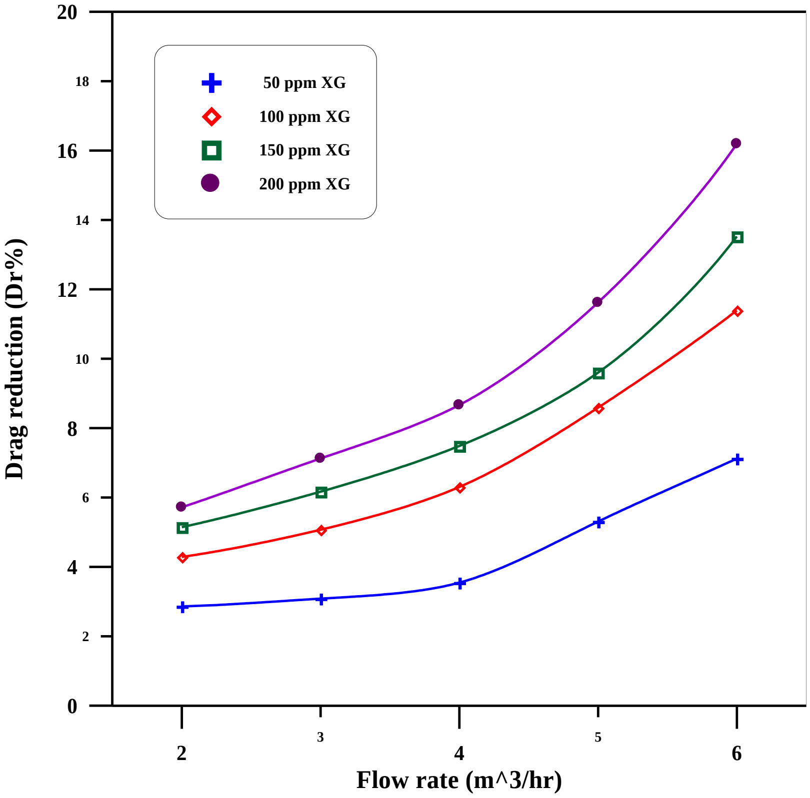

Figure 4.7, Percent drag reduction vs. flow rate for four selected concentrations of Xanthan Gum (XG).

4.3 Trisodium Polyphosphate (STPP)

Trisodium polyphosphate (STPP) is used usually as a builder in the detergent compounding to remove the hardness of water by elimination of the soluble Calcium and Magnesium salts by forming insoluble compounds.

The effectiveness of Trisodium polyphosphate (STPP) as drag-reducing agent was examined for the first time in water turbulent flow, as function of concentration and flow rate, as show in figures 4.8 and 4.9. Percentage drag-reduction was found to increase by increasing the additive concentration and solution flow rate.

Figure 4.8 shows the dependence of percentage drag reduction on STPP concentration of 50-200 ppm at different flow rates ranging between 2-6 m^3/hr. This figure indicates that high concentrations and high turbulency are a predominant for efficient drag-reduction. Those, about 5.7% drag-reduction is achieved by addition of 50 ppm additive at 6 m^3/hr flow rate. While the corresponding value is about 11.4 % by using 200 ppm additive. Furthermore, the effect of flow rate is clearly shown in figure 4.9 by adding 200 ppm STPP at flow rates 2, 3, 4, 5, and 6m^3/hr.

It is worthy to explain that STPP is more less effective as drag-reducer than the flexible long chain polyethylene oxide and polyacryl amide polymers which achieve above 31% drag-reduction at 100 ppm concentration compared with about 11% for 200 ppm STPP additive.

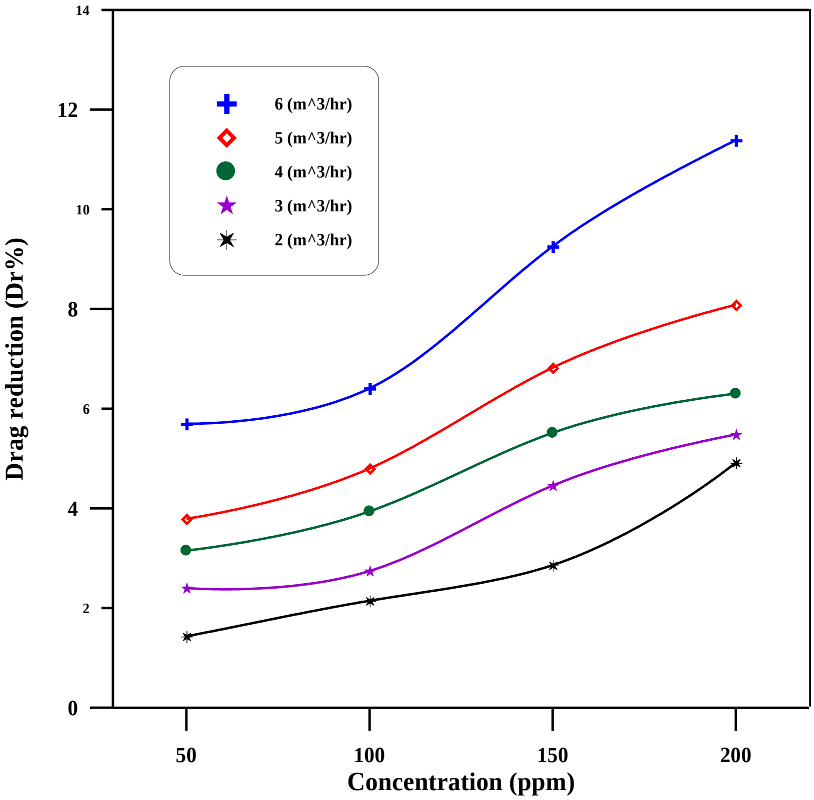

Figure 4.8, Percent drag reduction vs. flow rate for different concentrations of STPP

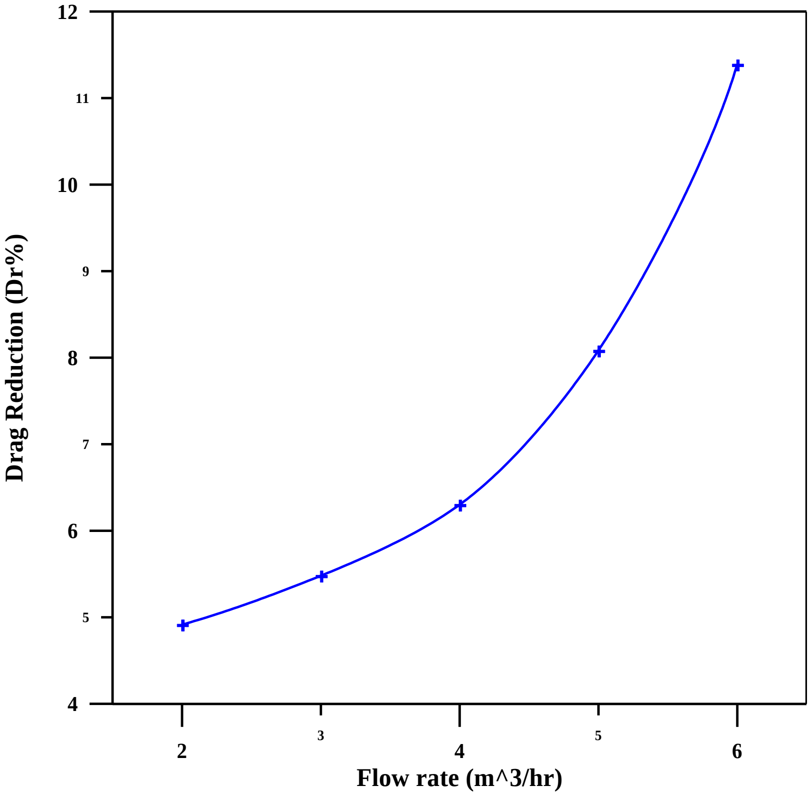

Figure 4.9, Effect of flow rate on percentage drag-reduction of 200 ppm STPP additive.

4.4 Suspended Particles Additives

4.4.1 Clay (Kaolin)

Experiments were performed to evaluate the drag reduction effectiveness of certain Kaolin type of natural clay additive suspended in water. The study aimed also to investigate the effect of minor amounts of clay as additive in reducing the energy requirement for discharge of river water and in possible sprinkler irrigation system as well as to increase the throughout area of converge.

The results of effectiveness of clay on percentage drag reduction are plotted in figure 4.10, for additive concentration ranging from 50-500 ppm. It is clear that clay acts as efficient drag reducer for flowing water . A gradually increase of percentage drag reduction is observed as clay additive concentration increases. It is possible that the presence of non – settling slurries (turbidity) aqueous solution of clay influence the viscosity of flowing water. Therefore, the increasing in the drag reduction effectiveness in existing of clay is consistent with the observed changes in solution viscosity (88).

Furthermore clay acts as in case of surfactant to form rod-like micelles. The drag-reducing properties could be explained by the interaction of clay micelles with the waters, which allows the turbulence to be suppressed (37).

Figure 4.10 shows clearly that clay concentration is predominant to get maximum drag-reduction. The data for 6 m^3/hr flow rate are 5.3%, 10.1%, 12.8% for concentrations 50, 250, 500 ppm respectively. It seems to be that clay additive concentrations above 250 ppm and water flow rate 5-6 m^3/hr are suitable conditions to get expectable drag-reduction effectiveness.

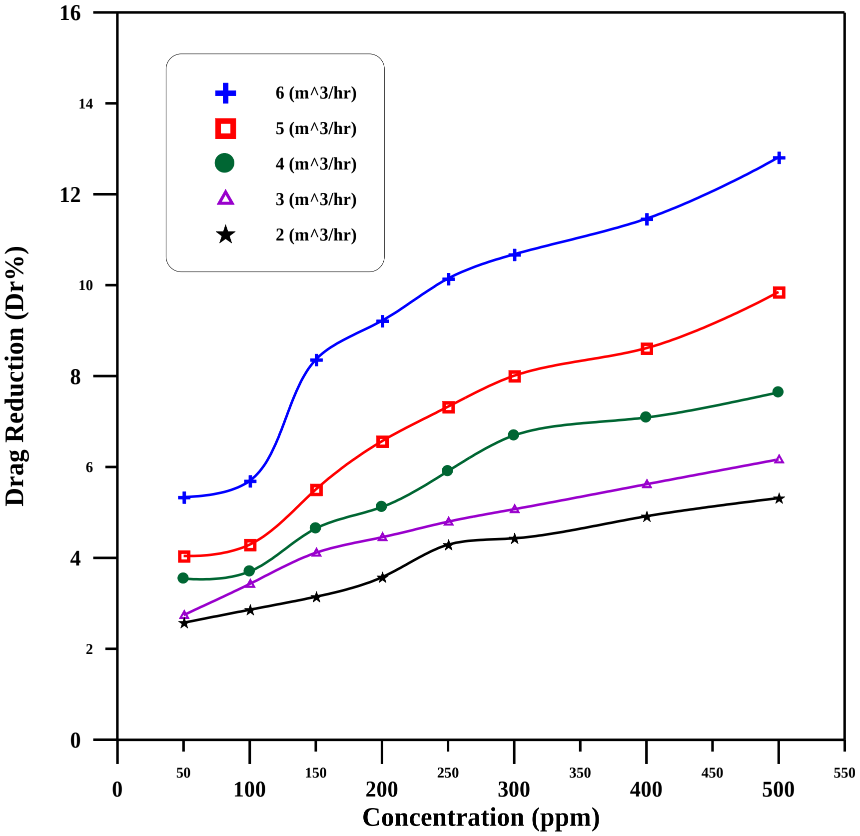

Figure 4.10, Percent drag reduction vs. Clay concentrations of different flow rates

Furthermore, the effect of flow rate on drag-reduction performance of suspended clay additive is demonstrated in details in figure 4.11, increase the fluid flow rate means increasing the degree of turbulence inside the pipe, this will provide a better media to clay as drag-reducer to be more effective.

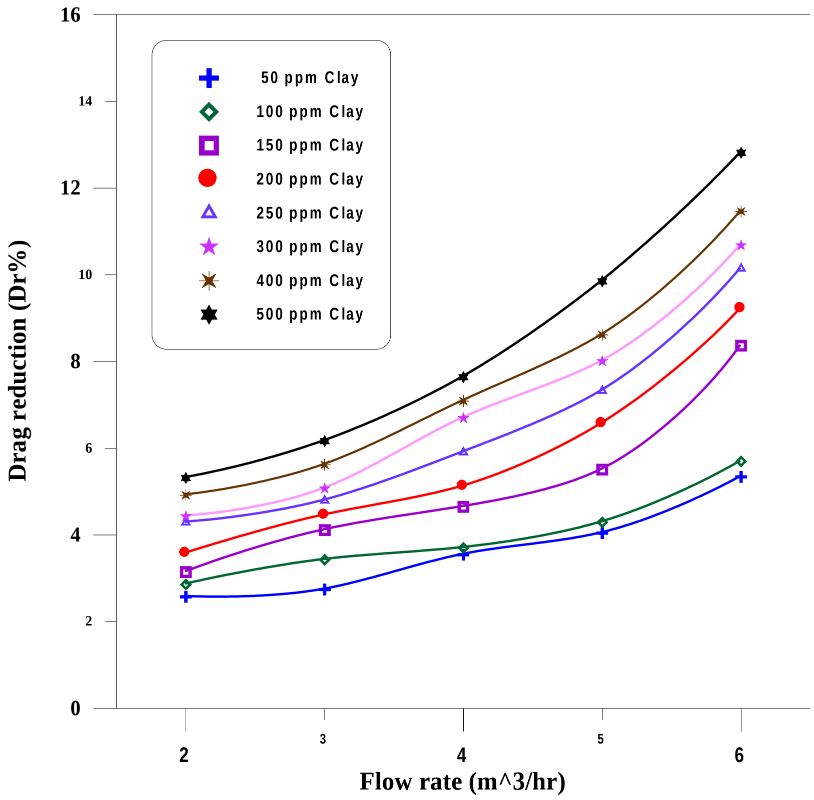

Figure 4.11, Effect of flow rate on effectiveness of Clay as drag-reduction agent

4.4.2 Alum

The experiments were performed to study the ability of Alum in reducing the drag forces of turbulent water flows. Since, Alum is used widely in water treatment systems for coagulation and precipitation of suspended particles, such as clays and sand. The drag- reduction performance of Alum was investigated for concentrations ranging 50-1000 ppm and 2-6 m^3/hr water flow rates, as illustrated in figures 4.12 and 4.13. The results indicate that Alum acts as an efficient drag-reducer agent, reaching about 25.2 % drag-reduction at maximum conditions of 1000 ppm additive and 6 m^3/hr flow rate.

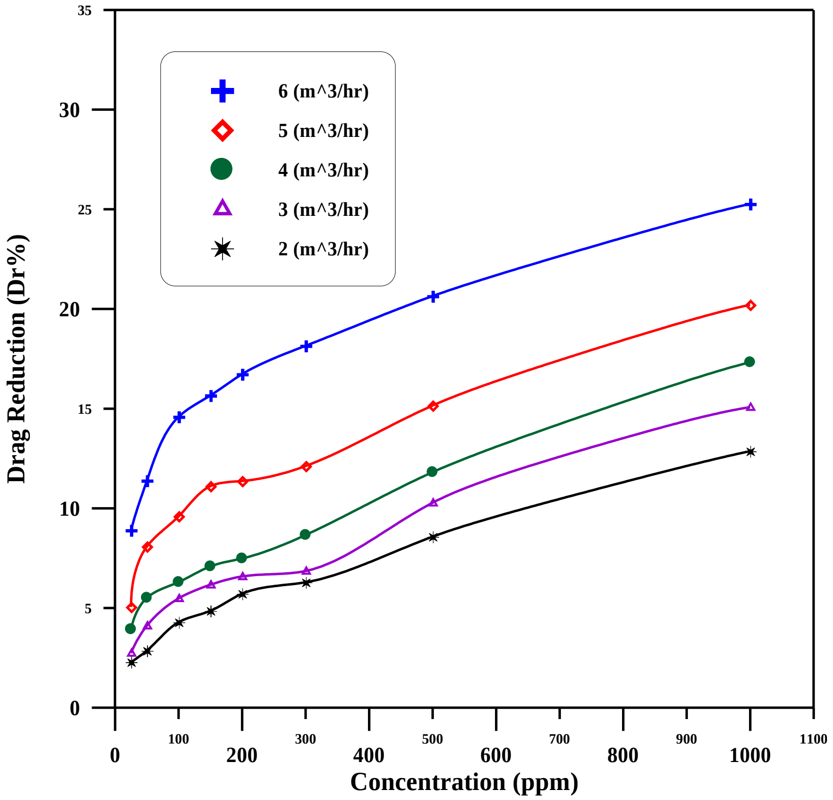

Figure 4.12, Percent drag reduction vs. flow rate for different concentrations of Alum

The effectiveness of Alum as drag-reducer is influenced largely by increasing the additive concentration and degree of turbulency, as it is expected for the most drag-reducing agents. Furthermore, figures 4.12 and 4.13 show that concentrations above 300 ppm Alum and water flow rates 4-6 m^3/hr are necessary to get acceptable drag-reduction values within the studied conditions.

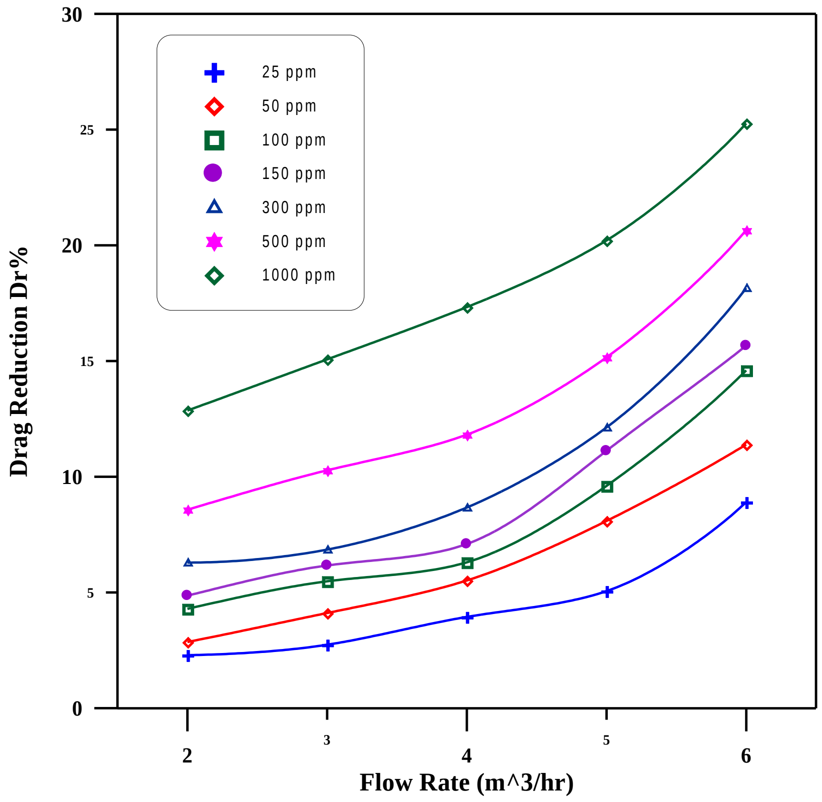

Figure 4.13, Percent drag reduction vs. concentrations for different flow rates of Alum,

It is worthy to notice that Alum additive is more efficient drag-reducer agent than clay, both as suspended particles. The maximum percentage drag-reduction for alum was about 25.2% compared with about 13 % for Clay at specified flowing condition. This could be attributed to lowering the solution viscosity in presence of Alum more than the existent of Clay (88), since Alum forms gels, which is mixed with the water in colloid form, and probably to the interactions between above particles in water turbulence flow. Furthermore, it is possible that the gelling of Alum acts as in case of surfactants to form rod-like micelles (88). The drag-reducing properties could be also explained by the interaction of Alum micelles with the water, which allows the turbulence to be suppressed.

4.5 Effectiveness of Binary Additives

4.5.1 Polymers and Clay

The screening study was performed to evaluate the drag-reduction performance of polymeric additives in presence of clay as suspended particles. The concentration of polymers was 50 ppm for each Polyethylene Oxide and Polyacrylamide and 100 ppm for Xanthan Gum. The polymeric additive was mixed with different concentrations of Clay, ranging between 100 and 500 ppm, as illustrated in figures 4.14, 4.15, and 4.16 for the above polymers respectively. The result show that percentage drag-reduction increases slightly with increasing the concentration of Clay as combined additive. It seems to be that both additives enhance the reduction of drag forces in a synergistic manner in turbulent water flow.

Figure 4.14 shows that the drag-reduction effectiveness of mixed additive with PEO polymer increases with increase the Clay values, which reach about 21.7% for pure 50 ppm PEO in 1.25 " pipe at 6.0 m^3/hr flow rate, but it increases to about 23.8 % by adding 500 ppm of Clay to the same solution . In other words 9.0% drag-reduction increase is achieved as shown in figure 4.17. The values for 50 ppm polyacrylamide additive were about 17 % for pure PAAM jumped to about 20% adding 500 ppm Clay at the same flowing conditions. This means a 9.4 % increase in percentage drag reduction as shown in figure 4.17. Similarly, about 11.4 % drag-reduction was achieved for 100 ppm pure Xanthan Gum agent increases to about 14% with combination with 500 ppm Clay, leading to more than 19 % increase, which is the highest value compared with flexible polymers, as shown in figure 4.17.

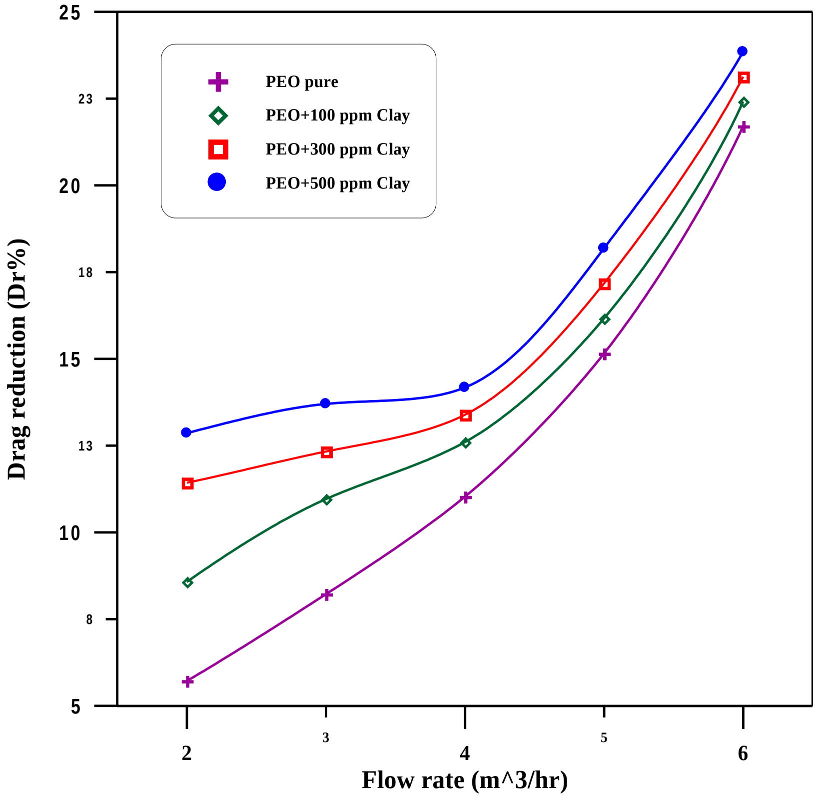

Figure 4.14, Percent drag reduction vs. flow rate for 50 ppm of PEO combined with different concentrations of Clay

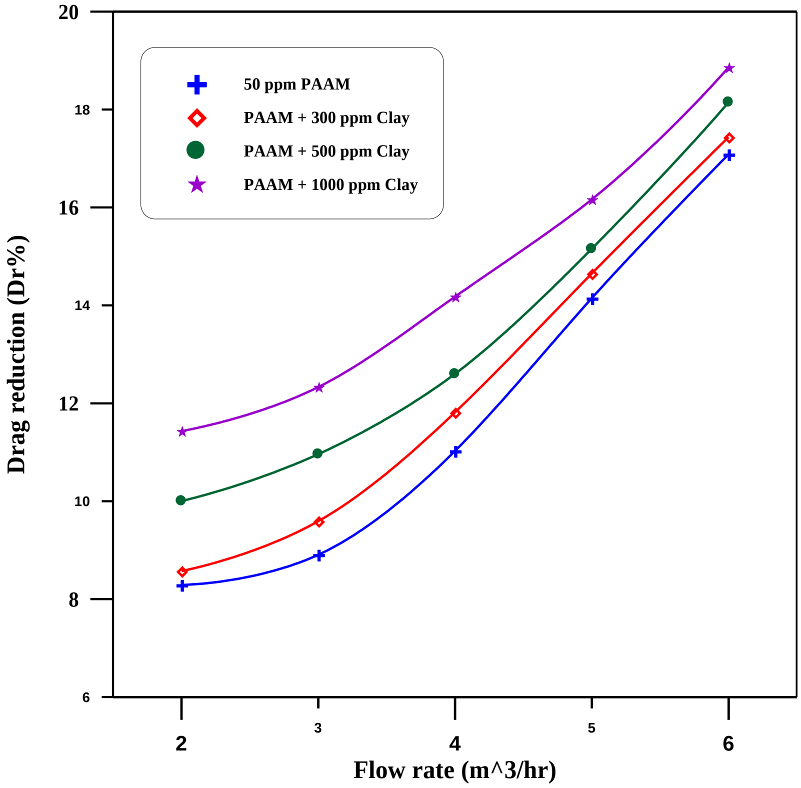

Figure 4.15, Percent drag reduction vs. flow rate for 50 ppm of PAAM combined with different concentrations of Clay

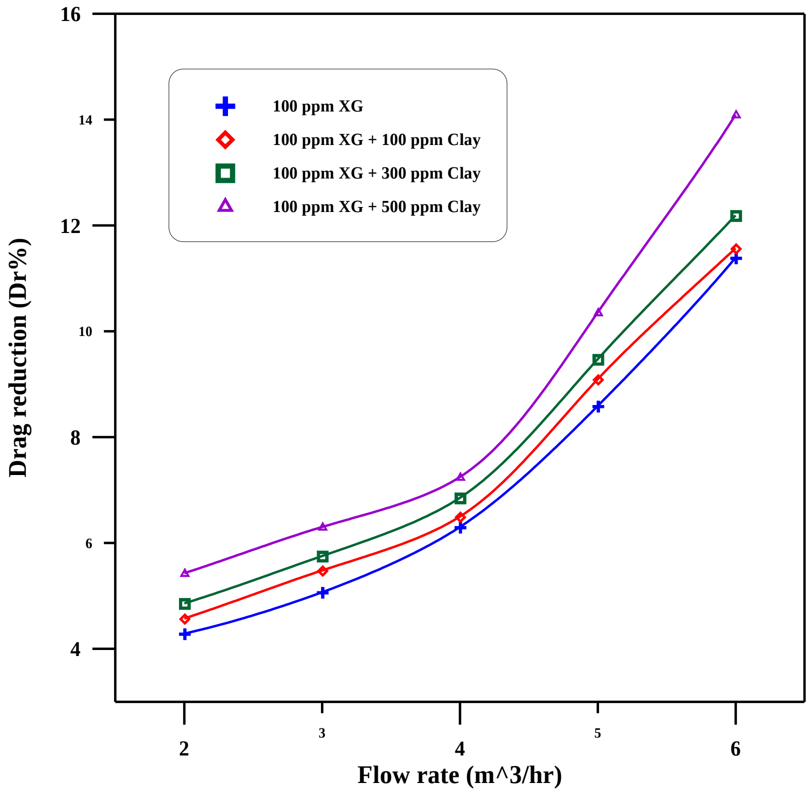

Figure 4.16, Percent drag reduction vs. flow rate for 50 ppm of XG combined with different concentrations of Clay

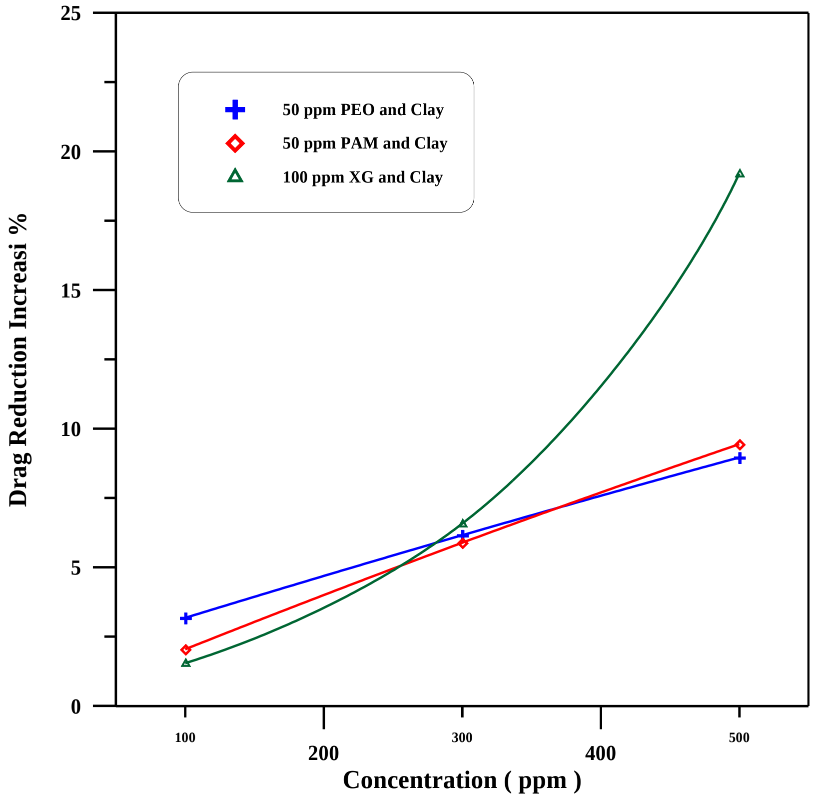

Figure 4.17, Percent drag reduction increase vs. concentration of clay for different polymers at $6m^3/hr$

4.5.2 Polymer and Alum

Figures 4.18, 4.19, and 4.20, show the results of combined effect of Polyethylene Oxide, Polyacrylamide, and Xanthan Gum additives with different concentrations of Alum on percentage drag-reduction respectively. 50 ppm of each, Polyethylene Oxide and Polyacrylamide and 100 ppm of Xanthan Gum were used in the experimental study. The polymeric additive was mixed with different concentrations of Alum, ranging between 100 to 500 ppm. The drag-reduction effectiveness of these polymers is improved by combination with Alum, as it was observed previously with clay as combined additives.

The results of percentage increase of drag-reduction are illustrated in figure 4.21 for the three polymers combined with Alum at 6.0 m^3/hr solution flow rates. The 100 ppm Alum enhances the drag-reduction ability of PEO, PAAM, and XG giving 15, 6, and 3% respectively. While, at 500 ppm Alum as combined additive, an increase of about 10, 9, and 19%, for the three considered polymers respectively. Furthermore, the results indicate clearly that higher concentration (i.e. 500 ppm) of Alum affected more the ability of XG as drag reducer additive. While the low concentration (i.e. 100 ppm), of Alum with 50 ppm PEO is more efficient combined additive than with 500 ppm Alum. Moreover, the increase of Alum from 100 ppm to 500 ppm has a little effect on effectiveness of PAAM as drag-reducer agent, as shown in figure 4.21. The effect of combined binary polymeric additives with Alum could be attributed to the different molecular interaction of such additives.

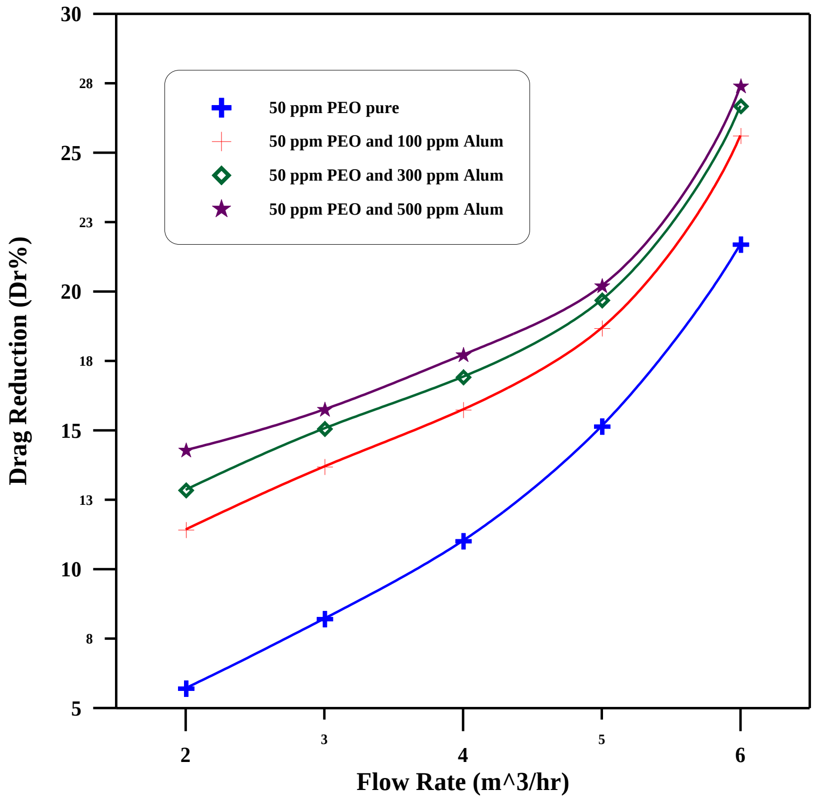

Figure 4.18, Percent drag reduction vs. flow rate for different concentrations of Alum at 50 ppm PEO

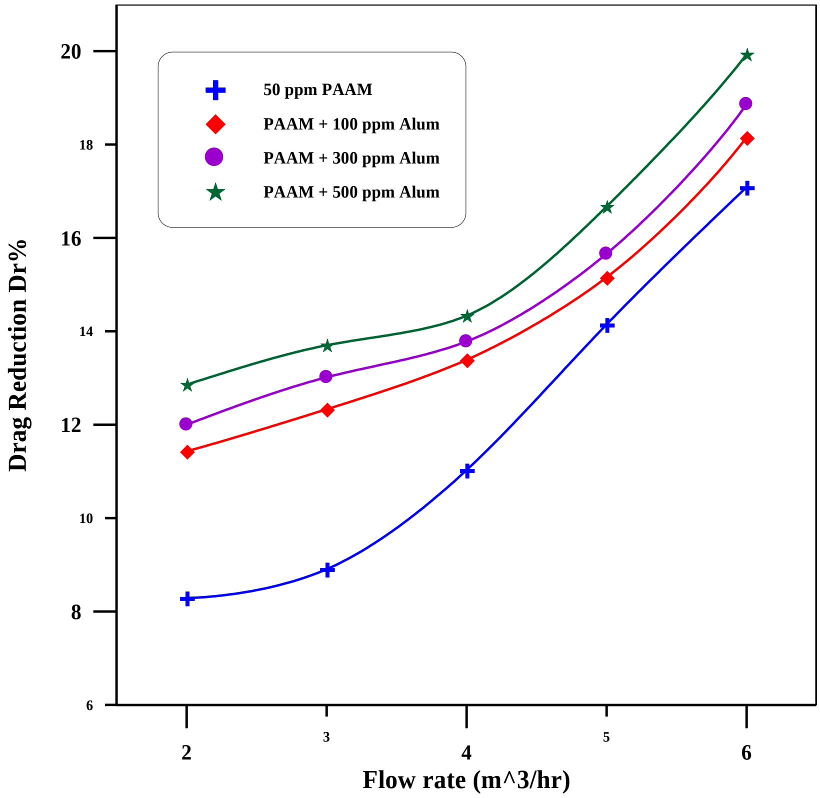

Figure 4.19, Percent drag reduction vs. flow rate for different concentrations of Alum at 50 ppm PAAM

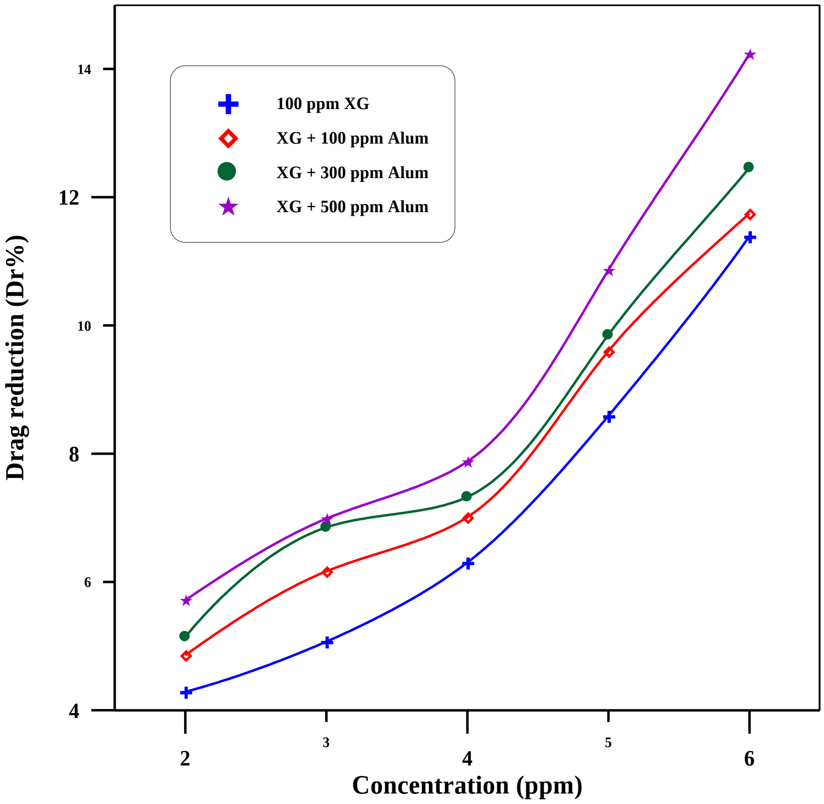

Figure 4.20, Percent drag reduction vs. flow rate for different concentrations of Alum at 100 ppm XG

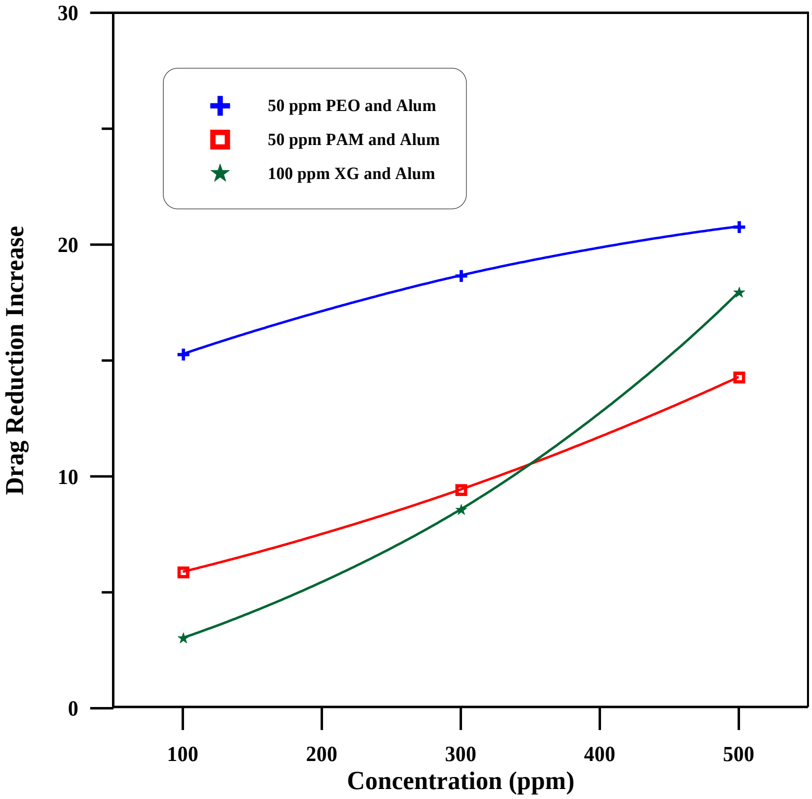

Figure 4.21, Percent drag reduction increase vs. concentrations of Alum for different Polymers at 6 m^3/hr

4.5.3 Binary mixtures with STPP

As it was observed porously, both Xanthan Gum and Alum additives possess a good drag-reduction ability, reaching about 11.4% and 14.6 % respectively for 100 ppm concentration and 6.0 m^3/hr solution flow rate, while about 6.2 % was obtained for Trisodium Polyphosphate (STPP) at the same flowing condition, In this section an attempt was made to use binary mixtures of STPP with XG and Alum to investigate there drag-reduction effectiveness. The results are illustrated in figures 4.22 and 4.24 respectively, at different concentrations of STPP and solution flow rates.

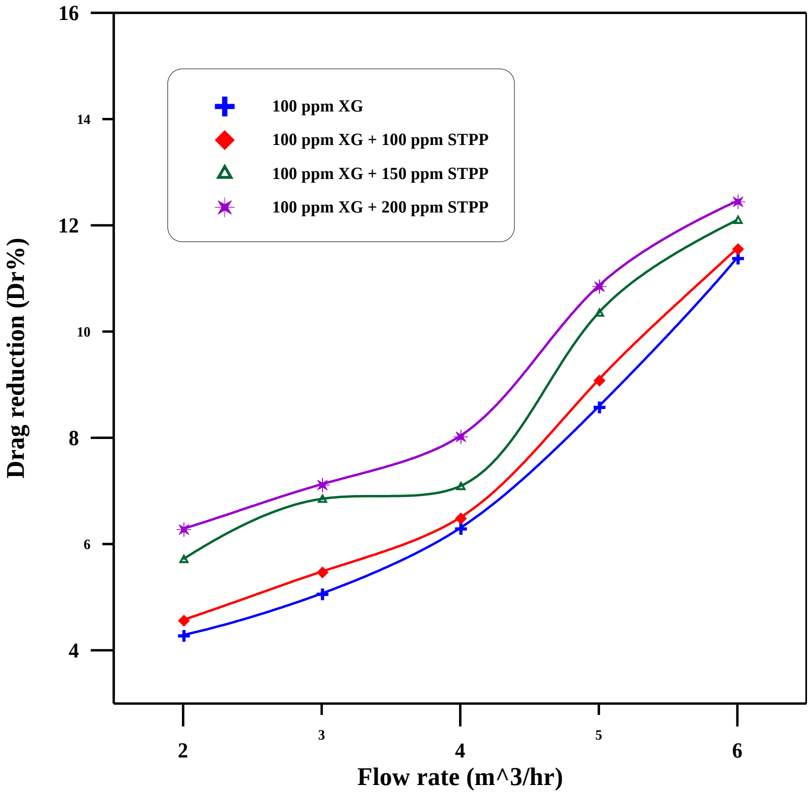

Figure 4.22, Percent drag reduction vs. flow rate for 100 ppm Xanthan Gum (XG) and different concentrations of (STPP)

Figure 4.22 shows that a slight increase of drag-reduction effectiveness of XG with increasing STPP concentration, reaching a maximum percentage increase of about 8.6% by 200 ppm STPP, as illustrated in figure 4.23. The improvement at drag-reduction effectiveness could be attributed to increase of total additives concentration. Therefore it can be concluded that the addition of STPP to XG has no positive effect on its drag-reduction effectiveness.

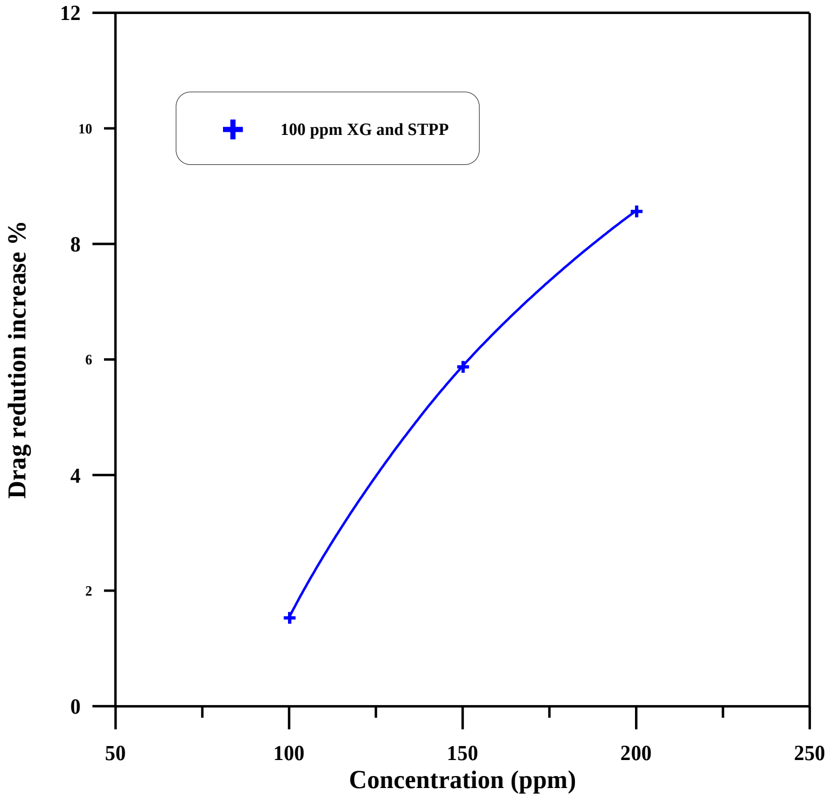

Figure 4.23, Percent drag reduction increase vs. concentrations for 100 ppm XG and different concentrations of STPP at 6m3/hr

Figure 4.24 shows the percentage drag reduction of 200 ppm STPP mixed with different concentrations of Alum, up to 1000 ppm. A gradual increase of percent drag reduction is observed with increasing of Alum concentration, reaching about 29% for 1000 ppm Alum as illustrated in figure 4.25. Moreover, the results in figure 4.24 indicate that %Dr for each 200 ppm STPP and 100 ppm Alum alone is about 11.2 and 14.6 respectively, while a mixture of both additives resulted is about 10.2 % drag reduction, which is lowes than for individual additives. Similar drag-reduction for single 500 ppm Alum is 20.6 % drops to about 13.2% by mixing with 200 ppm STPP which is significant lower than for pure Alum additive. It can be concluded that STPP acts as inhibitor to the performance of Alum is reducer. The inhibited effect of STPP on drag-reduction effectiveness of Alum can be attributed to its molecular configuration of the former in presence of STPP as electrolyte molecules. A similar effect was observed by Rochetort and Middeman (88) by addition the ionic sodium chloride to Xanthan Gum.

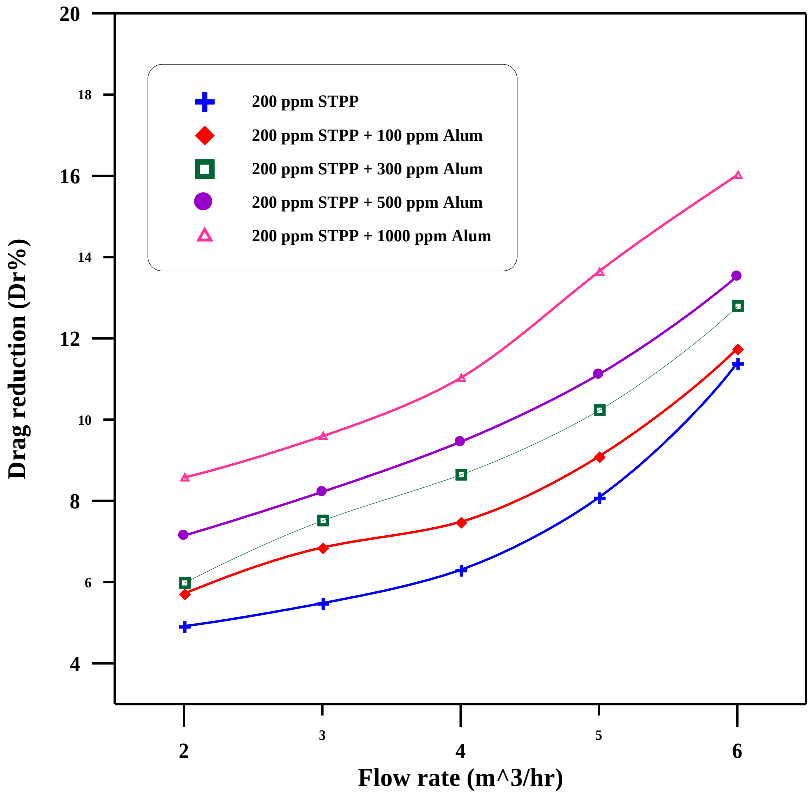

Figure 4.24, Percent drag reduction vs. flow rate for 200 ppm of STPP and different concentration of Alum

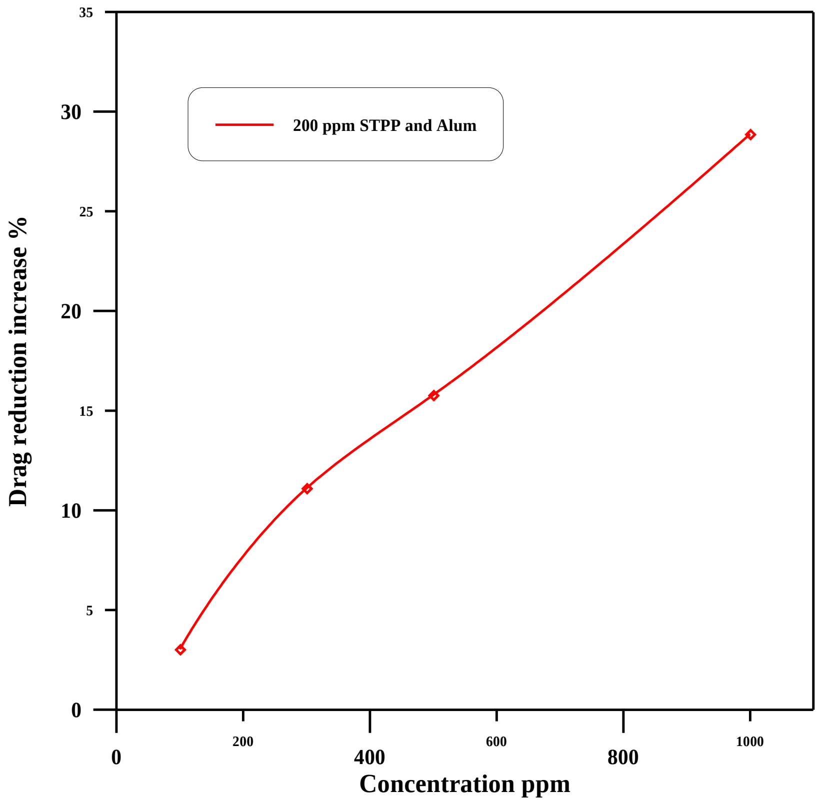

Figure 4.25, Percent drag reduction increase vs. concentrations for 200 ppm STPP and different concentrations of Alum at 6m3/hr

4.6 Friction Factor

It is desired to represent the effectiveness of the considered additives as drag-reducers in the form of fanning friction factor versus solvent Reynolds number. The use of Reynolds number based on the solvent viscosity and pipe diameter provides a direct indication of the degree of turbulent drag-reduction.

The fanning friction factor (f) was calculated from the experimental data based on pressure drop measurements as in equation 2.24, which was described previously in section 2.6.2

$$f = \frac{\Delta P.D/4L}{\rho v^2/2} \qquad \ldots (2.24)$$

Figure 4.26 represents the relationship between *f* and Re for Polyethylene Oxide, Polyacrylamide, Xanthan Gum, Trisodium polyphosphate, Alum, and Clay additives treated water at two concentrations of 50 and 100 ppm. While figure 4.27 illustrates friction factor data for PEO mixed with Alum and Clay and figure 4.28 for PAAM mixed Alum and Clay also.

Friction factor values for Clay and Alum as suspended particles in flowing water shift toward Blasius asymptotes. While the experimental data points for the more effective, flexible polymers PEO and PAAM positioned in the direction of lowering the friction factor towards Virk asymptote which represent maximum limits of drag-reduction; as shown in figure 4.26. Furthermore, as Re increases the corresponding *f* decreases for all additive types. Consequently, the give higher drag-reduction values as compared with lower Reynolds number flows.

The addition of Alum and Clay to PEO or PAAM agents result in low friction factors towards Virk asymptote, indicating an enhancement effect of such suspended of the polymeric agents, as shown in figures 4.27 and 4.28 for PEO and PAAM respectively. Alum acts more as activator than Clay.

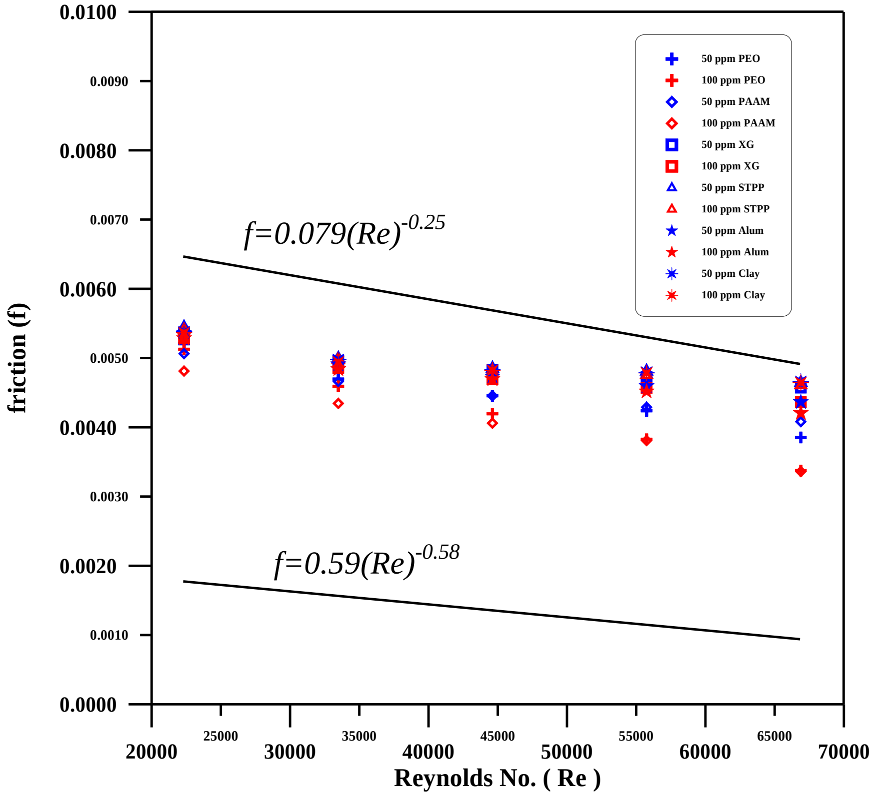

Figure 4.26, the fanning friction factor vs. Reynolds number for polymers, STPP, Alum, and Clay

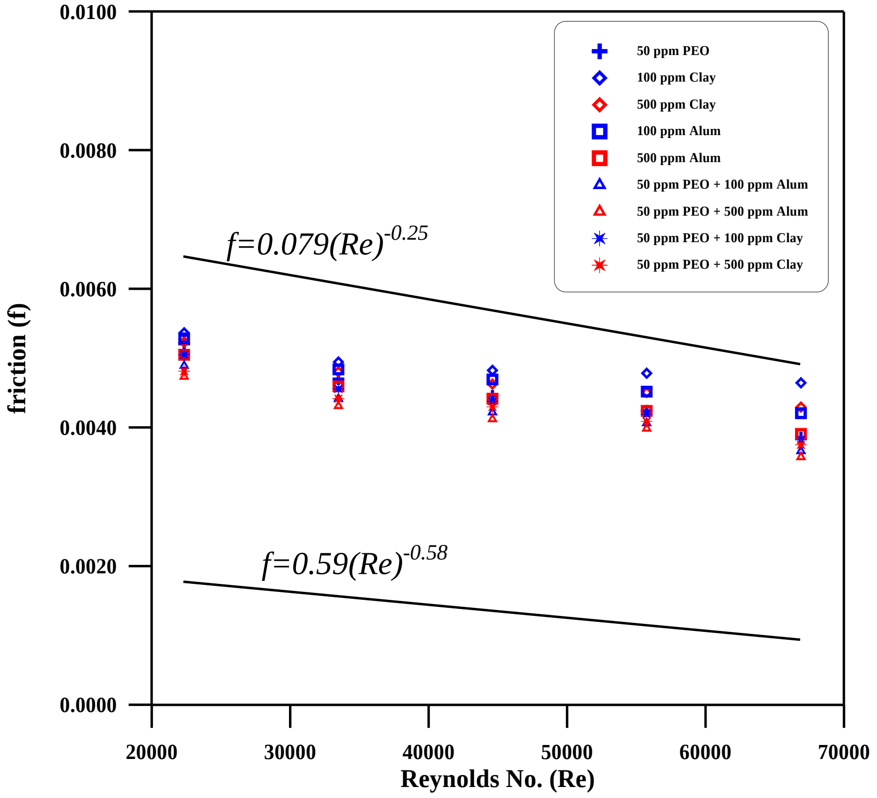

Figure 4.27, the fanning friction factor vs. Reynolds number for PEO mixed with Alum and Clay

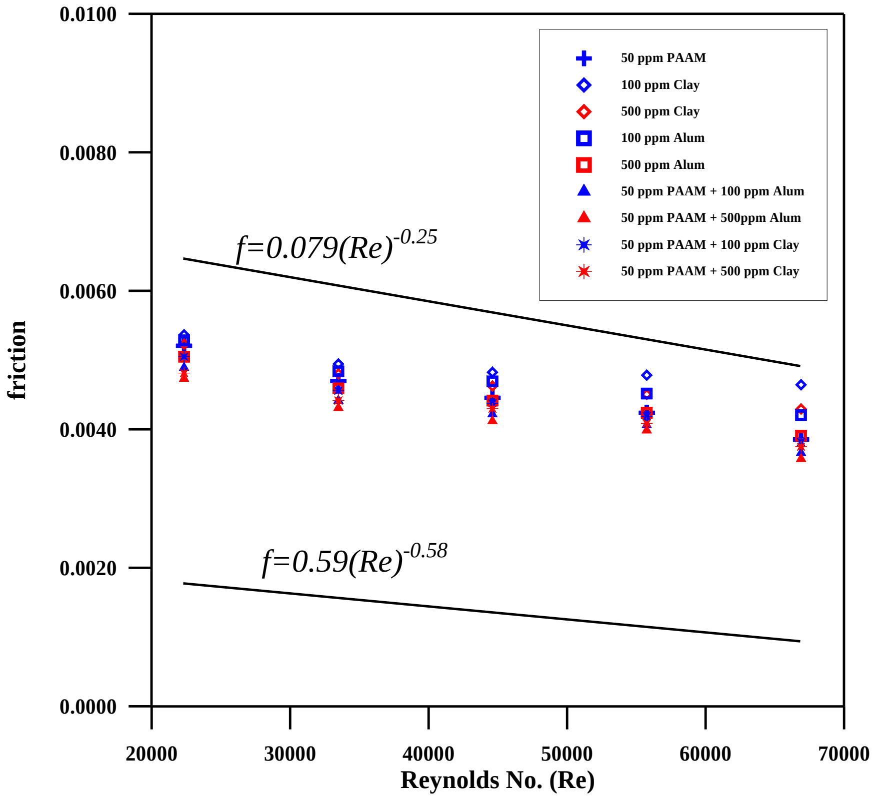

Figure 4.28 the fanning friction factor vs. Reynolds number for PAAM mixed with Alum and Clay

CHAPTER FIVE

CONCLUSIONS AND RECOMMENDATIONS

5.1 Conclusions

1. Flexible polymers, Polyethylene Oxide and Polyacrylamide gave higher percent drag-reductions than the rigid Xanthan Gum and suspended particles at their optimum concentrations. This could be attributed to the higher molecular weight and the longer polymer chains of flexible polymers which provide more chance for entanglement and interaction with the turbulent water flow.
2. Alum was found for the first time to behave good drag-reducing agent. Percentage drag-reduction was found to increase by increasing the particles concentration and solution flow rate. It is drag-reduction properties could be explained by the interaction of Alum gels with the water, which allows the turbulence to be suppressed.
3. It was found for the first time that Trisoduim Polyphosphate (STPP) is an efficient drag-reducer agent. Percentage drag-reduction was found to increase at high flow rates. STPP is used usually to eliminate the water hardness in detergent formulation. Those the drag-reduction ability of STPP could be attributed partially to remove Calcium and Magnesium salts, which act usually as inhibitor for drag-reduction performance.
4. Drag reduction effectiveness of PEO and PAAM can be slightly improved by combined mixing with Clay, Alum or STPP.
5. Admixtures of Xanthan Gum with Clay, Alum or STPP cause a noticeable increase in the drag-reduction preoperties.

6. For all additive types used lower friction factors are obtained for high additive concentrations and high Reynolds number.

5.2 Recommendations

1. Studying the time dependence of Clay, Alum and STPP additives.
2. Further work can be carried out by using different type of solid particles to improve the drag reduction effectiveness of polymers or surfactants.
3. The effects of pipe roughness and diameter need to be investigated on drag-reduction effectiveness of suspended particles and STPP as additives.
4. The effect at pipe fittings such as elbows and values on drag-reduction of suspended particles needs to be studied.
5. Performance of full-scale tests of drag reduction additives in the field before selecting the finial additive is an important step for an accurate simulation of the whole process of drag-reduction.

REFERENCES

1. **BA Toms**, Proceedings of International Congress on Rheology, Vol. II, pp. 135, North Holland, Amsterdam (1949).

2. **GT Pruitt and HR Craw**, Westco Research Final Report on Contract 60530-8250 to Naval Ordinance Test Station (1963).

3. **JG Savins**, Soc. Petrol. Eng. 4, 203 (1964).

4. **JW Hoyt and AG Fabula**, Proceedings – 10th International Towing Tank Conference, Teddington (1963).

5. **JW Hoyt and AG Fabula**, Proceedings – 5th Symposium on Naval Hydrodynamics, Bergen, Norway, Office of Naval Research ACR-112, 947 (1964).

6. **AG Fabula**, JW Hoyt and HR Crawford, Bull. Am. Phys. Soc. 8 (1963).

7. **JW Hoyt, Trans**. Am. Soc. Mech. Engrs, J. Basic Engng 94, 258 (1972).

8. **Zakin J.L.,** "Some recent developments in surfactant drag reduction", www.turbulence–control.gr.jp, may (2005).

9. Ali E.S., Ph.D Thesis, University of Technology, 1996.

10. **W.M. Kulicke and M. Kötter** "Drag Reduction phenomenon with Special Emphasis an Homogeneous polymer Solution in polymer characterization/ polymer Solution", Adv. Polymer Sci. 89, 1-68, (1989).

11. **K.R Sreenivasan and C.M. whith** "The Onset of Drag

Reduction by Dilate polymer Additives, and The Maximum Drag Reduction Asymptote”, J. Fluid Mech., 409, pp1490164, (2000).

12. **Zeiad A.R Aswad et. Al**, “Optimizing Viscous Flow in pipes Through Improved Flow Conditions and Chemical Injections. Vol.2, (2001).
13. **T. Dujmovich, A. Gallegos and C. Phillips,** “Drag – Reducer Improve Throughput”, Penn Well Corporahou, (2005**).**
14. **H. Thiel,.** Turbulent flow of heterogeneous polymer solution in aritically roughed pipe. “Drag Reduction Fluid Flow” Editors, R.H Sellin and R.T. Moses, 1989.
15. **Sarem, A.M.,** "Drag Reduction Does Not Always Increase with Increased Flow Velocity ", Sco.Pet.Eng., Paper 4338, June (1973).
16. **Al- Qamaje , Haidar Moafag Taofeag,** " Flow Increase in Turbulent Fluid Flow by Using Drag Reduction Agents ", M.Sc thesis in Chemical Engineering of Al Nahrain University, 2006.
17. **Choi, H.J. and M.S. jhon, ,** " Polymer – Induced Turbulent Drag Reduction Characteristics of Polyisobutylene in a rotating disk apparatus", Ind. Eng. Chem. Res. 35, 2993-2998, (1996).
18. **Sarah E.Morgan**," Water Soluble Copolymers Macromolecular Drag Reduction", a review of predictive theory. Prog. Polym sci. Vol.15, p. 507-549, 1990.
19. **www.exxonmobil.com** "Vistanex polyisobutylene Properties and Applications".2005.

20. **Ambari, C. Desloais,** "The Influence of polymer Additives on Velocity and Temperature field" IUTAM Sump. Editor B. Gampert, P. 437, 1984.

21. **Truong V.-T., "**Drag Reduction Technologies**",** DSTO-GD-0290

22. **DW Dodge and AB Metzner,** AIChE J. 5, 189 (1959).

23. **Rana Z. Mohammed,** "The Effect of Surface Active Agents on Friction Reduction in pipe liquid flow" M.Sc. Thesis, Nahrain University, Baghdad, 2008.

24. **H. Usui and T. Saeki,** "Drag Reduction and Heat transfer Reduction by Cationic Surfactant", J. Chem. Eng. Japan, Vol. 26, No. 1, 1993.

25. **GE Gadd,** Nature 212, 1348 (1966).

26. **Savins, J.G., and Seyer, F.A.,** "Drag Reduction Scale- Up Criteria", The Physics of Fluids, Vol.20, No.10, Pt.2, s86-s81, October (1977).

27. **Brod, M., B.C. Deane, and F. Rossi,** "Field Experience with the Use of Additives in the Pipeline of Waxy Crudes", J.Intst.Petrol., 57(554), pp 110-116, (1971).

28. **Motier, J.F.,** "Polymeric Drag Reducers", Pipeline and Gas Journal, p. 32-379, June (1985).

29. **Zakin J.L.** "Existence Of Two Types Of Drag Reduction In Pipe Flow Of Dilute Polymer Solutions", Chem. Eng. Sci., 6, pp. 381, (1967).

30. **RG Shaver and EW Merrill,** AIChE J., 5, 181 (1959).

31. **Kim C.A., J.TKim, K.Lee, H.J.Choi, and M.S.Jhon**," A High-Precision Rotating Disk Apparatus For Drag Reduction Characteristic", Polymer Testing, 20 pp 43-48, (2001).

32. **E.Bilgen and R. Boulos**, Trans. Of the CSME 1, 25, (1972).

33. **Shenoy A. V.**, J. Colloid and Polymer. Sci, 262, 319, (1984).

34. **Diver D.R. and Bakhtiyarov S.I.**, J. Non – Newtonian Fluid Mech. 12, 113.

35. **Zagustin, A., and K. Zagustin,** “Mechanics of Turbulent Flow in Sediment Laden Streams,” *Inter. Cong. Hydr. Res*., Kyoto, Japan, B33, **2**, (1969).

36. **Mahmood, K.,** “Flow in Sand-Bed Channels,” Ph.D. Thesis , Colorado State-University, (Feb. 1971).

37. **A.H. Dhiaa,** "Friction Reduction caused by the addition of additives into a turbulent flow" M.Sc. Thesis, Nahrain University, Baghdad, 2008.

38. **Berge, B. K. and Solsvik, O.:** “Increased Pipeline Throughput using Drag Reducer Additives (DRA)”, SPE, 36835, 22-25, October 1996.

39. **M Tsutahara and M Sakamoto,** Trans. of the JSME Series B 61, 2088 (1995).

40. **McCormick ME and Bhattacharyya R,** Nav. Eng. J. 85, 11 (1973).

41. **VG Bodgevich, AR Evseev and AG Malyuga,** Second International Conference on Drag Reduction, Cambridge (England), BHRA, P. 25 (1977).

42. **CL Merkle and S Deutsch, in** "Frontiers in experimental fluid mechanics" vol. 46 (M Gad-el-Hak, ed), pp 291 (1989).

43. **NK Madavan,** S Deutsch and CL Merkle, Phys. Fluids 27, 356 (1984).

44. **S Pal, S Deutsch and CL Merkle**, Phys. Fluids A1, 1360 (1989).

45. **S Deutsch and J Castano,** Phys. Fluids 29, 3590 (1986).

46. **S Deutsch and S Pal,** Phys. Fluids A2, 2943 (1990).

47. **Kato H, M Miyanaga and Y Haramoto, in** "Cavitation and gas-liquid flow in fluid machinery and devices" (TJ O'Hern, JH Kim, WB Morgan eds), FED vol 190, ASME, New York, p. 185 (1994).

48. **Kato H, M Miyanaga and H Yamaguchi, in** "Advances in multiphase flow" (A Serizawa, T Fukano and J Bataille eds.), Proceedings of the Second International Conference on Multiphase Flow, Kyoto, Elsevier, Amsterdam, p 85 (1995).

49. **Guin MM, Kato H and Takahashi Y, in "**Proceedings of the International Symposium on Seawater Drag Reduction", Newport, Rhode Island, pp. 155 (July 1998).

50. **Guin MM, Kato H,** H Yamaguchi, M Maeda and M Miyanaga, J. Mar. Sc. Technol. 1, 241 (1996).

51. **S Pal, CL Merkle and S Deutsch,** Phys. Fluids 31, 744 (1988).

52. **Madavan NK, CL Merkle and S Deutsch,** Trans. Of the ASME, 107, 370 (1985).

53. **MO Kramer,** J. Aero. Sci. 24, 459 (1957).

54. **MO Kramer,** J. Amer. Soc. Naval Engrs. 72, 25 (1960).

55. **S Taneda and H Honji**, Report of Research Institute of Applied Mechanics 15, 1 (1967).

56. **PBS Lissaman and GL Harris,** AIAA Paper No. 69-164 (1969).

57. **M Gad-el-Hak,** Appl. Mech. Rev. 49, S147 (1996).

58. **Carpenter PW and Garrard AD,** J. Fluid Mech. 155, 465 (1985).

59. **Gaster M, in** “Turbulence Management and Relaminarisation” (HW Liepmann and R Narasimha eds), Springer-Verlag, Berlin, p. 285 (1988).

60. **AE Dixon, AD Lucey and PW Carpenter**, AIAA Journal 32, 256 (1994).

61. **PW Carpenter and PJ Morris,** J. Fluid. Mech. 218, 172 (1990).

62. **PW Carpenter,** AIAA Journal 31, 1187 (1993).

63. **KH Chung, PhD Thesis** “Composite Compliant Coatings For Drag Reduction Utilizing Low Modulus High Damping Silicone Rubber” (1985).

64. **Benjamin TB,** J. Fluid. Mech. 9, 513 (1960).

65. **MT Landahl,** J. Fluid. Mech. 13, 609 (1962).

66. **C.M. DaRocha, L.G. Patruyo, N.E. Ramirez, A.J. Muller,** A.E. Saez, Polym. Bull. 42 (1999) 109.

67. **Z. Matras, Przepływ cieczy Tomsa w przewodach kołowych, Cracow** University of Technology, 1984 23.

68. **J.M Coulson J.M. and Richardson J.F**., "Chemical Engineering", Vol.1, (1985).Pergamon Press.

69. **Robert H.Perry, Don w.Green, James O.Malony,** "Perry's Chemical Engineers' Hand Book", Seventh Edition, (1998).

70. **Jain A.K., "Fluid mechanics",** Khanna publishers, Delhi (1993).

71. MOODY, L. F.: *Trans. Am. Soc. Mech. Engrs.* 66 (1944) 671. Friction factors for pipe flow.

72. **Schlichting H.,** Boundary Layer Theory,6th Edition , McGraw-Hill , New York,(1987).

73. **Wilson, N.W., and Azad R.S.,** " A Continuous Prediction Method for Fully Developed Laminar, Transition and Turbulent Flows in Pipes", J. Applied Mech., 42, pp. 51-57 (1975).

74. **Jackob, M.and Jan, D.T.,** " Drag reduction by polymer additives in turbulent pipe flow: laboratory and numerical experiments", Ph.D thesis, (2002).

75. **Bottural L.,** "Friction Factor Correlations", Cryosoft, www.cryosoft.com, Feb.6 (1999).

76. **Virk, P.S.,** "Drag Reduction Fundamentals ", Aiche J., Vol.21, Mo.4, p.625-656, July (1975).

77. Mysels K.J., "Early experiences with Viscous Drag Reduction", ***Chem. Eng. Prog. Symp. Seri***., 67 (111), pp. 45–49 (1971).

78. **Wilson, N.W., and Azad R.S.,** " A Continuous Prediction Method for Fully Developed Laminar, Transition and Turbulent Flows in Pipes", J. Applied Mech., 42, pp. 51-57 (1975).

79. **Holland F.A.,** "Fluid for Chemical Engineering", Edward Arnold, 1st Edition (1973).

80. **Nada, S. Al – Z.,** “Thermal Stability of Polymer” M.S.C Thesis University of Baghdad, Petroleum of Engineering, (1989).

81. **E.D Burger, W.R. Munk and H.A. Wahi,** "Flow Increase in the Trans-Alaska Pipeline Using a Polymeric Drag Reducing Adduitives", J. petroleum Tech. Feb. 1982, 377-386**.**

82. **N. S. Berman, et al.** An observation of the effect of the integral scale on drag-reduction, AICHE J. 24, 124, 1978**.**

83. **Manfred B., Jan G.D., Gary H.L. and Grey J.H.,** "TAPS Experience Proves Flow Improvers can Raise Capacity", Pipeline and Gas J., Sep., pp. 43–46 (1982)**.**

84. **Slaiman I. N.,** "Effectiveness of Polyisobutylene Drag Reducing agent in Turbulent pipe flow" Ph.D Thesis, Nahrian University, 2007

85. **Rose G.D., Faster K.L, Slocum V.L. and Lenhart J.G.,** "Drag Reduction and Heat Transfer of Viscoelastic Surfactant Formulations", Paper (D.6) presented at the 3rd Int. conf. on drag reduction , Bristol, July (1984).

86. **N. S. Berman,** Flow tirae scales and drag reduction, phys. Fluids, IUTAM sgmp. 1977.

87. **Robert H.Perry, Don w.Green, James O.Malony**, "Perry's Chemical Engineers' Hand Book", Seventh Edition, (1998).

88. **W.E. Rochefort and S. Middeman,** "Relationship between Rheological Bahaviour and Drag-Reduction for dilute XG Solution", Drag reduction in fluid flow symposium, Editor R. Sellin and R.T. Moses, 1989.

APPENDICES

Appendix A

Table (A-1) Experimental data of pure water& PEO

Conc.	**Flow Rate (m^3/hr)**	**Reynolds No.**	**Dr %**	***f***
0	**6**	66836.72157	-	0.00493591
	5	55697.26797	-	0.00500828
	4	44557.81438	-	0.00501935
	3	33418.36078	-	0.00512913
	2	22278.90719	-	0.00553314
10 ppm	**6**	66836.72157	8.541	0.004514336
	5	55697.26797	6.566	0.004679438
	4	44557.81438	5.118	0.004762458
	3	33418.36078	4.110	0.004918325
	2	22278.90719	2.857	0.005375058
20 ppm	**6**	66836.72157	10.676	0.004408954
	5	55697.26797	8.081	0.004603563
	4	44557.81438	6.299	0.004703179
	3	33418.36078	4.795	0.004883191
	2	22278.90719	3.714	0.005327639
30 ppm	**6**	66836.72157	14.235	0.004233285
	5	55697.26797	10.101	0.004502395
	4	44557.81438	7.480	0.004643901
	3	33418.36078	5.479	0.004848107
	2	22278.90719	4.286	0.005295989
40 ppm	**6**	66836.72157	17.438	0.004075188
	5	55697.26797	12.121	0.004401228
	4	44557.81438	8.661	0.004584622
	3	33418.36078	6.846	0.004777992
	2	22278.90719	4.857	0.005264395
50 ppm	**6**	66836.72157	21.708	0.003864424
	5	55697.26797	15.152	0.004249427
	4	44557.81438	11.024	0.004466015
	3	33418.36078	8.219	0.004707569
	2	22278.90719	5.714	0.005216976

Conc.	**Flow Rate (m^3/hr)**	**Reynolds No.**	**Dr %**	***f***
75 ppm	**6**	66836.72157	26.406	0.003632535
	5	55697.26797	19.343	0.00403953
	4	44557.81438	12.992	0.004367234
	3	33418.36078	9.041	0.004665408
	2	22278.90719	6.571	0.005169557
100 ppm	**6**	66836.72157	31.423	0.0033849
	5	55697.26797	23.384	0.003837145
	4	44557.81438	16.220	0.00420521
	3	33418.36078	10.274	0.004602166
	2	22278.90719	7.143	0.005137907

Table (A-2) Experimental data of pure water& PAAM

Conc.	**Flow Rate (m^3/hr)**	**Reynolds No.**	**Dr %**	***f***
0	**6**	66836.72157	-	0.00493591
	5	55697.26797	-	0.00500828
	4	44557.81438	-	0.00501935
	3	33418.36078	-	0.00512913
	2	22278.90719	-	0.00553314
10 ppm	**6**	66836.72157	11.459	0.00437
	5	55697.26797	9.596	0.004528
	4	44557.81438	7.087	0.004664
	3	33418.36078	6.164	0.004813
	2	22278.90719	5.714	0.005217
25 ppm	**6**	66836.72157	14.591	0.004216
	5	55697.26797	10.859	0.004464
	4	44557.81438	9.449	0.004545
	3	33418.36078	8.219	0.004708
	2	22278.90719	7.143	0.005138
50 ppm	**6**	66836.72157	17.082	0.004093
	5	55697.26797	14.141	0.0043
	4	44557.81438	11.024	0.004466
	3	33418.36078	8.904	0.004672
	2	22278.90719	8.286	0.005075
100 ppm	**6**	66836.72157	31.673	0.003373
	5	55697.26797	23.737	0.003819
	4	44557.81438	18.898	0.004071
	3	33418.36078	15.068	0.004356
	2	22278.90719	12.857	0.004822

Table (A-3) Experimental data of pure water& XG

Conc.	**Flow Rate (m^3/hr)**	**Reynolds No.**	**Dr %**	***f***
0	**6**	66836.72157	-	0.00493591
	5	55697.26797	-	0.00500828
	4	44557.81438	-	0.00501935
	3	33418.36078	-	0.00512913
	2	22278.90719	-	0.00553314
50 ppm	**6**	66836.72157	7.117	0.004584601
	5	55697.26797	5.303	0.004742691
	4	44557.81438	3.543	0.004841497
	3	33418.36078	3.082	0.004971043
	2	22278.90719	2.857	0.00537505
100 ppm	**6**	66836.72157	11.388	0.004373815
	5	55697.26797	8.586	0.004578278
	4	44557.81438	6.299	0.004703169
	3	33418.36078	5.068	0.004869163
	2	22278.90719	4.286	0.005296005
150 ppm	**6**	66836.72157	13.523	0.004268422
	5	55697.26797	9.596	0.004527689
	4	44557.81438	7.480	0.004643885
	3	33418.36078	6.164	0.004812953
	2	22278.90719	5.143	0.005248578
200 ppm	**6**	66836.72157	16.192	0.004136681
	5	55697.26797	11.616	0.004426512
	4	44557.81438	8.661	0.004584601
	3	33418.36078	7.123	0.00476377
	2	22278.90719	5.714	0.00521696

Table (A-4) Experimental data of pure water& STPP

Conc.	**Flow Rate (m^3/hr)**	**Reynolds No.**	**Dr %**	***f***
0	**6**	66836.72157	**-**	0.00493591
	5	55697.26797	**-**	0.00500828
	4	44557.81438	**-**	0.00501935
	3	33418.36078	**-**	0.00512913
	2	22278.90719	**-**	0.00553314
50 ppm	**6**	66836.72157	5.694	0.004654863
	5	55697.26797	3.788	0.004818574
	4	44557.81438	3.150	0.004861258
	3	33418.36078	2.397	0.005006174
	2	22278.90719	1.429	0.005454095
100 ppm	**6**	66836.72157	6.406	0.004619732
	5	55697.26797	4.798	0.004767985
	4	44557.81438	3.937	0.004821736
	3	33418.36078	2.740	0.004988608
	2	22278.90719	2.143	0.005414572
150 ppm	**6**	66836.72157	9.253	0.004479208
	5	55697.26797	6.818	0.004666808
	4	44557.81438	5.512	0.004742691
	3	33418.36078	4.452	0.004900781
	2	22278.90719	2.857	0.00537505
200 ppm	**6**	66836.72157	11.388	0.004373815
	5	55697.26797	8.081	0.004603572
	4	44557.81438	6.299	0.004703169
	3	33418.36078	5.479	0.004848084
	2	22278.90719	4.914	0.005261225

Table (A-5) Experimental data of pure water& Clay

Conc.	**Flow Rate (m^3/hr)**	**Reynolds No.**	**Dr %**	***f***
0	**6**	66836.72157	-	0.00493591
	5	55697.26797	-	0.00500828
	4	44557.81438	-	0.00501935
	3	33418.36078	-	0.00512913
	2	22278.90719	-	0.00553314
50 ppm	**6**	66836.72157	5.338	0.004672429
	5	55697.26797	4.040	0.004805927
	4	44557.81438	3.543	0.004841497
	3	33418.36078	2.740	0.004988608
	2	22278.90719	2.571	0.005390859
100 ppm	**6**	66836.72157	5.694	0.004654863
	5	55697.26797	4.293	0.00479328
	4	44557.81438	3.701	0.004833593
	3	33418.36078	3.425	0.004953477
	2	22278.90719	2.857	0.00537505
150 ppm	**6**	66836.72157	8.363	0.004523122
	5	55697.26797	5.505	0.004732573
	4	44557.81438	4.646	0.004786166
	3	33418.36078	4.110	0.004918346
	2	22278.90719	3.143	0.005359241
200 ppm	**6**	66836.72157	9.217	0.004480965
	5	55697.26797	6.566	0.004679455
	4	44557.81438	5.118	0.004762452
	3	33418.36078	4.452	0.004900781
	2	22278.90719	3.571	0.005335527
250 ppm	**6**	66836.72157	10.142	0.004435294
	5	55697.26797	7.323	0.004641514
	4	44557.81438	5.906	0.00472293
	3	33418.36078	4.795	0.004883215
	2	22278.90719	4.286	0.005296005
300 ppm	**6**	66836.72157	10.676	0.004408946
	5	55697.26797	8.005	0.004607366
	4	44557.81438	6.693	0.004683407
	3	33418.36078	5.068	0.004869163

	2	22278.90719	4.429	0.005288101
Conc.	**Flow Rate (m^3/hr)**	**Reynolds No.**	**Dr %**	***f***
400 ppm	**6**	66836.72157	11.459	0.004370302
	5	55697.26797	8.611	0.004577013
	4	44557.81438	7.087	0.004663646
	3	33418.36078	5.616	0.004841058
	2	22278.90719	4.914	0.005261225
500 ppm	**6**	66836.72157	12.811	0.004303553
	5	55697.26797	9.848	0.004515042
	4	44557.81438	7.638	0.004635981
	3	33418.36078	6.164	0.004812953
	2	22278.90719	5.314	0.005239093

Table (A-6) Experimental data of pure water& Alum

Conc.	**Flow Rate (m^3/hr)**	**Reynolds No.**	**Dr %**	***f***
0	**6**	66836.72157	-	0.00493591
	5	55697.26797	-	0.00500828
	4	44557.81438	-	0.00501935
	3	33418.36078	-	0.00512913
	2	22278.90719	-	0.00553314
25 ppm	**6**	66836.72157	8.897	0.004496774
	5	55697.26797	5.051	0.004755338
	4	44557.81438	3.937	0.004821736
	3	33418.36078	2.740	0.004988608
	2	22278.90719	2.286	0.005406668
50 ppm	**6**	66836.72157	11.388	0.004373815
	5	55697.26797	8.081	0.004603572
	4	44557.81438	5.512	0.004742691
	3	33418.36078	4.110	0.004918346
	2	22278.90719	2.857	0.00537505
100 ppm	**6**	66836.72157	14.591	0.004215725
	5	55697.26797	9.596	0.004527689
	4	44557.81438	6.299	0.004703169
	3	33418.36078	5.479	0.004848084
	2	22278.90719	4.286	0.005296005
150 ppm	**6**	66836.72157	15.658	0.004163029
	5	55697.26797	11.111	0.004451806
	4	44557.81438	7.087	0.004663646
	3	33418.36078	6.164	0.004812953
	2	22278.90719	4.857	0.005264387
200 ppm	**6**	66836.72157	16.726	0.004110332
	5	55697.26797	11.364	0.004439159
	4	44557.81438	7.480	0.004643885
	3	33418.36078	6.575	0.004791875
	2	22278.90719	5.714	0.00521696
300 ppm	**6**	66836.72157	18.149	0.00404007
	5	55697.26797	12.121	0.004401217
	4	44557.81438	8.661	0.004584601
	3	33418.36078	6.849	0.004777822

	2	22278.90719	6.286	0.005185342

Conc.	Flow Rate (m^3/hr)	Reynolds No.	Dr %	*f*
500 ppm	**6**	66836.72157	20.641	0.003917112
	5	55697.26797	15.152	0.004249451
	4	44557.81438	11.811	0.004426512
	3	33418.36078	10.274	0.004602167
	2	22278.90719	8.571	0.005058871
1000 ppm	**6**	66836.72157	25.267	0.00368876
	5	55697.26797	20.202	0.003996508
	4	44557.81438	17.323	0.004149855
	3	33418.36078	15.068	0.00435625
	2	22278.90719	12.857	0.004821736

Appendix B

Table (B-1) Experimental data of PEO and Clay

Conc.	**Flow Rate (m^3/hr)**	**Reynolds No.**	**Dr %**	***f***
50 ppm PEO	**6**	66836.72157	21.708	0.003864
	5	55697.26797	15.152	0.004249
	4	44557.81438	11.024	0.004466
	3	33418.36078	8.219	0.004708
	2	22278.90719	5.714	0.005217
50 ppm PEO + 100 ppm Clay	**6**	66836.72157	22.420	0.003829
	5	55697.26797	16.162	0.004199
	4	44557.81438	12.598	0.004387
	3	33418.36078	10.959	0.004567
	2	22278.90719	8.571	0.005059
50 ppm PEO + 300 ppm Clay	**6**	66836.72157	23.132	0.003794
	5	55697.26797	17.172	0.004148
	4	44557.81438	13.386	0.004347
	3	33418.36078	12.329	0.004497
	2	22278.90719	11.429	0.004901
50 ppm PEO + 500 ppm Clay	**6**	66836.72157	23.843	0.003759
	5	55697.26797	18.182	0.004098
	4	44557.81438	14.173	0.004308
	3	33418.36078	13.699	0.004427
	2	22278.90719	12.857	0.004822

Table (B-2) Experimental data of PAAM and Clay

Conc.	**Flow Rate (m^3/hr)**	**Reynolds No.**	**Dr %**	***f***
50 ppm PAAM	**6**	66836.72157	17.082	0.004093
	5	55697.26797	14.141	0.0043
	4	44557.81438	11.024	0.004466
	3	33418.36078	8.904	0.004672
	2	22278.90719	8.286	0.005075
50 ppm PAAM + 100 ppm Clay	**6**	66836.72157	17.438	0.004075
	5	55697.26797	14.646	0.004275
	4	44557.81438	11.811	0.004427
	3	33418.36078	9.589	0.004637
	2	22278.90719	8.571	0.005059
50 ppm PAAM + 300 ppm Clay	**6**	66836.72157	18.149	0.00404
	5	55697.26797	15.152	0.004249
	4	44557.81438	12.598	0.004387
	3	33418.36078	10.959	0.004567
	2	22278.90719	10.000	0.00498
50 ppm PAAM + 500 ppm Clay	**6**	66836.72157	18.861	0.004005
	5	55697.26797	16.162	0.004199
	4	44557.81438	14.173	0.004308
	3	33418.36078	12.329	0.004497
	2	22278.90719	11.429	0.004901

Table (B-3) Experimental data of XG and Clay

Conc.	**Flow Rate (m^3/hr)**	**Reynolds No.**	**Dr %**	***f***
100 ppm XG	**6**	66836.72157	11.388	0.004374
	5	55697.26797	8.586	0.004578
	4	44557.81438	6.299	0.004703
	3	33418.36078	5.068	0.004869
	2	22278.90719	4.286	0.005296
50 ppm XG + 100 ppm Clay	**6**	66836.72157	11.566	0.004365
	5	55697.26797	9.091	0.004553
	4	44557.81438	6.496	0.004693
	3	33418.36078	5.479	0.004848
	2	22278.90719	4.571	0.00528
50 ppm XG + 300 ppm Clay	**6**	66836.72157	12.189	0.004334
	5	55697.26797	9.470	0.004534
	4	44557.81438	6.850	0.004676
	3	33418.36078	5.753	0.004834
	2	22278.90719	4.857	0.005264
50 ppm XG + 500 ppm Clay	**6**	66836.72157	14.093	0.00424
	5	55697.26797	10.354	0.00449
	4	44557.81438	7.244	0.004656
	3	33418.36078	6.301	0.004806
	2	22278.90719	5.429	0.005233

Table (B-4) Experimental data of PEO and Alum

Conc.	**Flow Rate (m^3/hr)**	**Reynolds No.**	**Dr %**	***f***
50 ppm PEO	**6**	66836.72157	21.708	0.003864
	5	55697.26797	15.152	0.004249
	4	44557.81438	11.024	0.004466
	3	33418.36078	8.219	0.004708
	2	22278.90719	5.714	0.005217
50 ppm PEO + 100 ppm Alum	**6**	66836.72157	25.623	0.003671
	5	55697.26797	18.687	0.004072
	4	44557.81438	15.748	0.004229
	3	33418.36078	13.699	0.004427
	2	22278.90719	11.429	0.004901
50 ppm PEO + 300 ppm Alum	**6**	66836.72157	26.690	0.003618
	5	55697.26797	19.697	0.004022
	4	44557.81438	16.929	0.00417
	3	33418.36078	15.068	0.004356
	2	22278.90719	12.857	0.004822
50 ppm PEO + 500 ppm Alum	**6**	66836.72157	27.402	0.003583
	5	55697.26797	20.202	0.003997
	4	44557.81438	17.717	0.00413
	3	33418.36078	15.753	0.004321
	2	22278.90719	14.286	0.004743

Table (B-5) Experimental data of PAAM and Alum

Conc.	Flow Rate (m^3/hr)	Reynolds No.	Dr %	*f*
50 ppm PAAM	**6**	66836.72157	17.082	0.004093
	5	55697.26797	14.141	0.0043
	4	44557.81438	11.024	0.004466
	3	33418.36078	8.904	0.004672
	2	22278.90719	8.286	0.005075
50 ppm PAAM + 100 ppm Alum	**6**	66836.72157	18.149	0.00404
	5	55697.26797	15.152	0.004249
	4	44557.81438	13.386	0.004347
	3	33418.36078	12.329	0.004497
	2	22278.90719	11.429	0.004901
50 ppm PAAM + 300 ppm Alum	**6**	66836.72157	18.861	0.004005
	5	55697.26797	15.657	0.004224
	4	44557.81438	13.780	0.004328
	3	33418.36078	13.014	0.004462
	2	22278.90719	12.000	0.004869
50 ppm PAAM + 500 ppm Alum	**6**	66836.72157	19.929	0.003952
	5	55697.26797	16.667	0.004174
	4	44557.81438	14.331	0.0043
	3	33418.36078	13.699	0.004427
	2	22278.90719	12.857	0.004822

Table (B-6) Experimental data of XG and Alum

Conc.	**Flow Rate (m^3/hr)**	**Reynolds No.**	**Dr %**	***f***
100 ppm XG	**6**	66836.72157	11.388	0.004374
	5	55697.26797	8.586	0.004578
	4	44557.81438	6.299	0.004703
	3	33418.36078	5.068	0.004869
	2	22278.90719	4.286	0.005296
50 ppm XG + 100 ppm Alum	**6**	66836.72157	11.744	0.004356
	5	55697.26797	9.596	0.004528
	4	44557.81438	7.008	0.004668
	3	33418.36078	6.164	0.004813
	2	22278.90719	4.857	0.005264
50 ppm XG + 300 ppm Alum	**6**	66836.72157	12.456	0.004321
	5	55697.26797	9.848	0.004515
	4	44557.81438	7.323	0.004652
	3	33418.36078	6.849	0.004778
	2	22278.90719	5.143	0.005249
50 ppm XG + 500 ppm Alum	**6**	66836.72157	14.235	0.004233
	5	55697.26797	10.859	0.004464
	4	44557.81438	7.874	0.004624
	3	33418.36078	6.986	0.004771
	2	22278.90719	5.714	0.005217

Table (B-7) Experimental data of XG and STPP

Conc.	**Flow Rate (m^3/hr)**	**Reynolds No.**	**Dr %**	***f***
100 ppm XG	**6**	66836.72157	11.388	0.004374
	5	55697.26797	8.586	0.004578
	4	44557.81438	6.299	0.004703
	3	33418.36078	5.068	0.004869
	2	22278.90719	4.286	0.005296
50 ppm XG + 100 ppm STPP	**6**	66836.72157	11.566	0.004365032
	5	55697.26797	9.091	0.004552983
	4	44557.81438	6.496	0.004693288
	3	33418.36078	5.479	0.004848084
	2	22278.90719	4.571	0.005280196
50 ppm XG + 150 ppm STPP	**6**	66836.72157	12.100	0.004338684
	5	55697.26797	10.354	0.004489748
	4	44557.81438	7.087	0.004663646
	3	33418.36078	6.849	0.004777822
	2	22278.90719	5.714	0.00521696
50 ppm XG + 200 ppm STPP	**6**	66836.72157	12.456	0.004321119
	5	55697.26797	10.859	0.004464453
	4	44557.81438	8.031	0.004616219
	3	33418.36078	7.123	0.00476377
	2	22278.90719	6.286	0.005185342

Table (B-8) Experimental data of STPP and Alum

Conc.	**Flow Rate (m^3/hr)**	**Reynolds No.**	**Dr %**	***f***
200 ppm STPP	**6**	66836.72157	11.388	0.004374
	5	55697.26797	8.081	0.004604
	4	44557.81438	6.299	0.004703
	3	33418.36078	5.479	0.004848
	2	22278.90719	4.914	0.005261
200 ppm STPP + 100 ppm Alum	**6**	66836.72157	11.744	0.004356
	5	55697.26797	9.091	0.004553
	4	44557.81438	7.480	0.004644
	3	33418.36078	6.849	0.004778
	2	22278.90719	5.714	0.005217
200 ppm STPP + 300 ppm Alum	**6**	66836.72157	12.811	0.004304
	5	55697.26797	10.253	0.004495
	4	44557.81438	8.661	0.004585
	3	33418.36078	7.534	0.004743
	2	22278.90719	6.000	0.005201
500 ppm STPP + 300 ppm Alum	**6**	66836.72157	13.523	0.004268
	5	55697.26797	11.111	0.004452
	4	44557.81438	9.449	0.004545
	3	33418.36078	8.219	0.004708
	2	22278.90719	7.143	0.005138
500 ppm STPP + 1000 ppm Alum	**6**	66836.72157	16.014	0.004145
	5	55697.26797	13.636	0.004325
	4	44557.81438	11.024	0.004466
	3	33418.36078	9.589	0.004637
	2	22278.90719	8.571	0.005059

الخلاصة

تم تصميم دراسة التجربة مبدئيا لتقييم فعالية الانواع المختلفة من المضافات كمعاملات تخفيض الاعاقة في كل من الاشكال الفردية والمزدوجة الخلط. ولما كانت المقارنة بين أكثر من نوع واحد من المضافات بالاخص بين المواد الكيمياوية التي تتحلل بالماء وبين المواد العالقة هي نادرة في الادب، فأن المضافات التي تم البحث عنها في العمل الحالي هي اوكسيد البوليثيلين (PEO) والبولي اكريلاميد (PAAM) مثل السلسة الطويلة المرنة من المركبات البوليمرية وصمغ زانثان (XG كبوليمر بوليساكاريد صلب طبيعي). علاوة على ذلك، فأن نوعا معينا من الطين الطبيعي (كاولين) نتج كمادة عالقة مضافة، بالاضافة الى سلفات الالمنيوم (الشب) وبوليي فوسفات الصوديوم الثلاثي (STPP) والتي استخدمت للمرة الاولى كمعامل تخفيض الاعاقة في الدراسة الحديثة.

تم دراسة تأثير تركيز المضافات لغاية ١٠٠ جزء في المليون لمادتي PEO و PAAM، و ٢٠٠ جزء في المليون لكل من XG و STPP و ٥٠٠ جزء في المليون للطين و ١٠٠٠ جزء في المليون للشب، وكلها بنسبة تدفق تصل الى ٦.٠ م^{٣}/ساعة في انبوب قطره الداخلي ١.٢٥ انج.

ان فعالية تقليل الاعاقة للبوليمر المرن، PEO و PAAM اكبر من تلك الخاصة بالمضافات المستخدمة الاخرى في اجمالي معدل التركيز في سرع تدفق مختلفة. وان اعلى تقليل أعاقة وصل الى ٣٢% تم الحصول عليه في ١٠٠ جزء في المليون في PEO و PAAM تمت اضافتها الى معدل جريان ٦.٠ م^{٣}/ساعة، ولذلك فقد تم اعتباره المعدل الامثل بين انواع المضافات. وقد أظهر كل من صمغ زانثان والطين والصوديوم الثلاثي فعالية معتدلة كمضاف لتقليل الاعاقة، بينما كان الالمنيوم اكثر فعالية عند التركيز ٥٠٠-١٠٠٠ جزء في المليون والتي اعطت نسبة اعاقة ٢١-٢٥% بسبب شكل المادة الغروية مع خليط الماء الذي يتسبب عنه تخفيض لزوجة المحلول.

وقد لوحظت زيادة طفيفة عند خلط الطين او الشب او STPP مع PEO و PAAM بينما تم الحصول على زيادة ظاهرة عند اضافة صمغ زانثان عند خلطه مع الطين او الشب او STPP.

وقد تم حساب معامل الاحتكاك من البيانات الجريبية التي تم ملاحظتها لكل المضافات التي درست في خط مختلف لبولي أثيلين اوكسايد والبولي اكريل اميد والشب عند رقم رينولد العالي بأتجاه الخط المقارب لـ Virk، والذي لم يتم الوصول اليه ابدا.

شكر وتقدير

الحمدلله الذي انعم علينا بتمام الصحة و فضلنا بنعمة العقل وزيننا بتاج العلم والصلاة والسلام على اشرف الخلق محمد وعلى آله وصحبة اجمعين.

اقف عاجزاً على التعبير عن مدى الشكر والامتنان الذي اود ان ابديه الى مشرفي الفاضل الاستاذ الدكتور جابر شنشول جمالي لما بذله من جهد وعناء لاخراج هذا النتاج العلمي بهذه الحله الغراء.

واتقدم بالشكر الجزيل الى استاذي الدكتور قاسم جبار سليمان رئيساً لقسم الهندسة الكيمياوية وجميع الكادر فيه لما بذلوه في مساعدتي لانجاز هذا العمل.

كما واتقدم بالشكر والاجلال الى والدي الكريمين اللذان حفوني بالدموع والدعاء كما واشكر اخي واخواتي اللذين لطالما كابدوا عناء البعد والفراق.

وشكري الجزيل لجميع زملائي الذين لم يقصرو في مساعدتي.

عمر جلاء يحيى

تخفيض المقاومة الإحتكاكية بسبب الإضافات المفردة والمشتركة

رسالة

مقدمة إلى كلية الهندسة في جامعة النهرين

وهي جزء من متطلبات نيل درجة ماجستير علوم

في الهندسة الكيمياوية

من قبل

عمر جلاء يحيى

بكالوريوس علوم في الهندسة الكيمياوية ٢٠٠٦

جمادى الآخرة ١٤٣٠هـ
حزيران ٢٠٠٩ م